

Continuous Evolution Pool : Taming Recurring Concept Drift in Online Time Series Forecasting

Tianxiang Zhan^{1,2}, Ming Jin², Yuanpeng He³, Yuxuan Liang⁴, Yong Deng¹, Shirui Pan²

¹University of Electronic Science and Technology of China, ²Griffith University, ³Peking University, ⁴Hong Kong University of Science and Technology (Guangzhou)

Recurring concept drift poses a dual challenge in online time series forecasting: mitigating catastrophic forgetting while adhering to strict privacy constraints that prevent retaining historical data. Existing approaches predominantly rely on parameter updates or experience replay, which inevitably suffer from knowledge overwriting or privacy risks. To address this, we propose the **Continuous Evolution Pool (CEP)**, a privacy-preserving framework that maintains a dynamic pool of specialized forecasters. Instead of storing raw samples, CEP utilizes lightweight statistical *genes* to decouple concept identification from forecasting. Specifically, it employs a **Retrieval** mechanism to identify the nearest concept based on gene similarity, an **Evolution** strategy to spawn new forecasters upon detecting distribution shifts, and an **Elimination** policy to prune obsolete models under memory constraints. Experiments on real-world datasets demonstrate that CEP significantly outperforms state-of-the-art baselines, reducing forecasting error by over 20% without accessing historical ground truth.

Date: January 29, 2026

Correspondence: ming.jin@griffith.edu.au, s.pan@griffith.edu.au

Code: https://github.com/ztxtech/cep_ts



1 Introduction

Accurate time series forecasting, a fundamental task in fields such as finance, energy management, traffic prediction, and environmental monitoring, empowers better decision-making, optimized resource allocation, and effective risk management [Jin et al. \(2024\)](#). However, in practical applications, online time series forecasting frequently encounters a substantial challenge known as *concept drift*. This is particularly critical as modern data often arrives in continuous streams, rendering traditional offline models trained on static historical data and making them quickly outdated. To maintain accuracy in such dynamic environments [Ditzler et al. \(2015\)](#), there is a crucial need for online forecasting models capable of incremental adaptation, eliminating the requirement for frequent and computationally expensive retraining. Concept drift refers to the change in the relationship between input variables and their true values over time. In the context of time series, as time elapses, the underlying patterns and behaviors governing the data can shift, making previously learned models less effective. *Recurring concept drift* is a particularly prevalent and intricate form of concept drift [Alippi et al. \(2013\)](#) in time series data, as shown in Figure 1(a). It is characterized by the periodic reappearance of certain concepts after a period of absence. For instance, seasonal patterns may cause similar consumption patterns to recur annually or monthly in electricity consumption time series. Crucially, these recurring patterns often encapsulate sensitive user behaviors or individual preferences such as household routines or mobility habits, *making strict privacy preservation paramount* when analyzing such recurrence [Johansson et al. \(2025\)](#). Nevertheless, as the time series evolves, the model may forget these previously encountered concepts during the non-recurrence periods, leading to a decline in the accuracy of online predictions as exemplified in Figure 1(b).

Various methods have been devised to tackle concept drift in the realm of online time series forecasting, but each has its own set of limitations. Methods based on Experience Replay (ER) [Chaudhry et al. \(2019\)](#), such as DER++ [Buzzega et al. \(2020\)](#), store historical information in a buffer for learning. However, in delayed

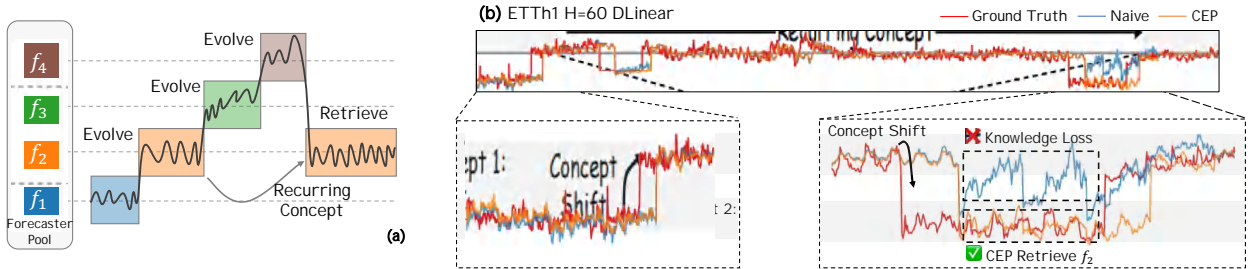


Figure 1 Concept recurrence is a notable phenomenon in time series data. For instance, in (a), the second concept recurs following the emergence of the fourth concept. During online updates and concept drifts, forecasters often suffer from forgetting previously learned concepts, as in (b). To address this challenge and effectively track recurring concepts, the Continuous Evolution Pool employs an evolving and retrieval strategy, assigning distinct forecasters to manage different concepts.

feedback settings, the experience pool quickly becomes outdated as the stored samples fail to reflect the latest data distribution, and the restricted memory size often leads to forgetting once-emerged concepts, thus degrading performance when adapting to the evolving data. FSNet Pham et al. (2023), drawing inspiration from the Complementary Learning Systems theory, tries to balance rapid adaptation to novel changes and the retrieval of past knowledge. In scenarios with sample delays Jhin et al. (2024), it encounters forecasting biases, making it harder to accurately capture the patterns in the time series. It also struggles to effectively learn relevant features during intricate concept drifts. OneNet Zhang et al. (2023) attempts to address concept drift by dynamically updating and integrating models through a reinforcement learning based approach. Nevertheless, its weight adjustment mechanism, which depends on recent prediction errors, fails due to information lag in delay scenarios, and it grapples with handling long-term dependencies in time series data, causing inaccuracies in predicting future trends.

Existing solutions for addressing concept drift in online time series forecasting mainly center around parameter updating techniques. These methods strive to make the model adapt to the changing data distribution by constantly adjusting the model’s parameters. While these methods can delay the forgetting of past concepts, they have multiple shortcomings. **First**, parameter updating might lead to the loss of some valuable previously learned knowledge. As the model tries to fit the new data, it could overwrite or distort information related to past concepts. **Second**, these methods generally overlook the exploration of effective knowledge retention mechanisms. Specifically, they do not explicitly store and utilize the knowledge of different concepts in a way that allows for efficient retrieval and reuse when those concepts reappear. **Third**, experiments on real-world datasets have demonstrated that neural networks can effectively learn under gradual distribution shifts without requiring complex adaptation mechanisms Read (2018). In the context of abrupt concept drift Read (2018), particularly in scenarios involving recurring concepts, there remains considerable room to improve the performance of existing methods. This is primarily because these methods have difficulty effectively capturing and adapting to sudden changes in data patterns, resulting in suboptimal forecasting accuracy. In light of these limitations, two crucial questions arise:

- **Q1:** Can we design a **decoupled adaptation** mechanism that uses *lightweight statistics* to filter macro distribution shifts, while leaving *micro-pattern variations* to the neural network’s gradient descent?
- **Q2:** How can we accurately identify distinct concepts and their recurrence, and manage these previously encountered concepts in a *resource-efficient* manner?

To address these limitations and effectively manage recurring concept drift in online time series forecasting, we propose the **C**ontinuous **E**volution **P**ool (CEP). This is a novel pooling mechanism designed to store multiple forecasters corresponding to different concepts. Its core idea involves partitioning samples from distinct distributions and continuously updating separate models for each evolving concept. When a new test sample arrives, CEP selects the forecaster in the pool that is nearest to this sample for prediction, concurrently learning from the features of its neighboring samples. If the neighboring samples are insufficient, this indicates the emergence of a new concept, prompting the evolution of a new model from the closest available sample. This new model is then added to the pool to retain knowledge of the emerging concept. Additionally, CEP employs

an elimination mechanism that removes outdated knowledge and filters noisy data, thereby maintaining high forecasting accuracy. Unlike complex feature extractors that risk overfitting to specific temporal patterns, CEP employs statistical moments (mean and variance) as Genes. This design is grounded in the statistical definition of concept drift as a distribution shift. By tracking low-order moments, CEP captures the fundamental regime changes while remaining robust to high frequency noise and computationally efficient for edge deployment. Unlike Time Series Foundation Models (TSFMs) that rely on massive pre-training resources [Ansari et al. \(2024\)](#), CEP focuses on **learning from scratch** in data isolated environments. We target privacy sensitive and hardware (e.g. network) constrained scenarios where large scale models are infeasible, prioritizing a lightweight, self-contained framework over a pre-trained generalist. The main contributions of this paper are as follows:

1. We identify recurring concept drift as a significant challenge in online time series forecasting, especially under delay feedback scenarios. Existing methods that rely on parameter updating frequently forget previously learned concepts during periods of non-recurrence and lack efficient mechanisms for knowledge retention. This results in reduced prediction accuracy when past concepts reappear.
2. We propose CEP, a pooling framework specifically designed to address recurring concept drift under delay feedback. By storing and retrieving forecasters associated with distinct concepts, CEP effectively mitigates knowledge loss inherent in traditional methods, enabling the model to leverage previously acquired knowledge more effectively.
3. Through extensive experiments involving multiple real-world datasets and various neural network architectures, we demonstrate that CEP substantially enhances online prediction accuracy in scenarios characterized by recurring concept drift. CEP consistently outperforms existing methods, particularly in managing complex time series data and delay scenarios.

2 Related Work

Concept Drift. Unlike conventional time series analysis, where concept drift might be less critical, it is a central concern in online time series forecasting. Suppose the input variables x and their ground truth y follow a distribution p_t over time as Equation (1). For two different time points t_1 and t_2 , the distribution shift can be formally defined by Equation (2) [Read \(2018\)](#).

$$(x, y) \sim p_t(x, y) \tag{1}$$

$$p_{t_1}(y|x) \neq p_{t_2}(y|x) \tag{2}$$

Concept drift was formally defined [Tsymbal \(2004\)](#), and emphasized for continuous adaptation in data streams [Read \(2018\)](#). Subsequent work includes the AdaRNN [Du et al. \(2021\)](#), which struggled with complex relationships, RevIN [Kim et al. \(2022\)](#) designed for distribution shift, and the exploration into online drift detection [Wan et al. \(2024\)](#). Despite these advancements, significant challenges remain in online time series forecasting, necessitating continuous research.

Online Time Series Forecasting. Unlike traditional methods, online time series forecasting requires continuous learning as new data arrives. Previous works [Huszár \(2018\)](#); [Kirkpatrick et al. \(2018\)](#) suffered from forgetting past knowledge and lacked rapid adaptation, rarely utilizing deep neural networks. As the field evolved, FSNet [Pham et al. \(2023\)](#) improved adaptation speed to recent data. To better capture complex relationships and address concept drift, OneNet [Zhang et al. \(2023\)](#) was introduced, combining cross-variable/cross-time modeling and online ensembling. Despite these advances, challenges persist, requiring ongoing research for improved performance and adaptability. Unlike Foundation Models that freeze parameters for zero-shot inference [Ansari et al. \(2024\)](#), online forecasting requires continuous parameter updates to capture evolving concepts. CEP focuses on this dynamic adaptation process with minimal memory footprint, distinct from the static inference paradigm of large models.

Distinctions from Other Drift Adaptation Approaches. While numerous methods address concept drift in various domains, several prominent approaches are not directly applicable to our specific scenario of recurring concept drift in online time series forecasting. Drift detectors (e.g., ADWIN Bifet and Gavalda (2009)) primarily focus on identifying *when* drift occurs but do not provide mechanisms for *how* to retain and manage independent forecasting models for different concepts, particularly in recurring scenarios. Tree-based models (e.g., ARF Gomes et al. (2017)), while effective for abrupt drift in classification tasks or single step forecasting, typically exhibit weaker performance in capturing long-range temporal dependencies compared to deep learning models, making them unsuitable for our multi-step forecasting requirements. Dynamically expanding continual learning methods Bifet and Gavalda (2009); Gomes et al. (2017); Elwell and Polikar (2011); Kim et al. (2024) are designed for classification tasks, and their mechanisms are difficult to transfer to our regression scenarios. Furthermore, unlike detectors that provide a binary signal of drift, CEP directly identifies *which concept the data resembles*, enabling *targeted retrieval of specialized knowledge rather than triggering a generic adaptation response*. This proactive, concept-centric mechanism is better suited for handling recurring drifts.

3 Methodology

In this section, we introduce the proposed CEP. It helps partition samples from different distributions, enabling the updating of different models for evolution. We describe how to utilize the dynamic evolution mechanism for the recurring concept scenario. For **Q1**, we introduce an evolution mechanism that assigns distinct concepts to specialized forecasters in Section 3.2 **Nearest Evolution**. For **Q2**, some adaptation techniques such as Elimination are introduced to manage the previously learned concepts in Section 3.2 **Forecaster Elimination**. The detailed notations are summarized in Appendix Table 4. A practical guide for choosing hyperparameters can be found in Appendix Table 15. Before introducing the CEP, we would like to state that *all the components of the method are indispensable*. This is crucial not only for forecasting accuracy but also for balancing **memory consumption** and **robustness** in practice.

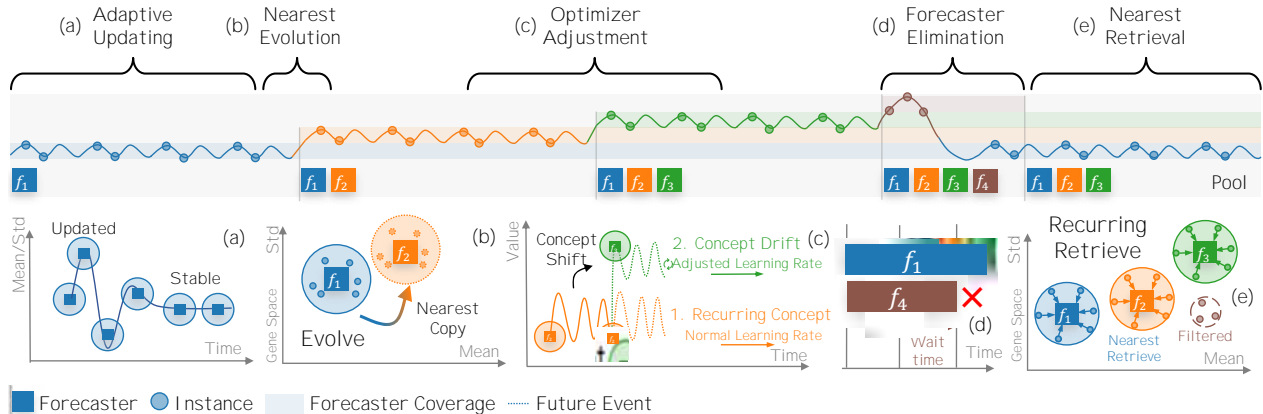


Figure 2 Illustration of the proposed CEP mechanism: (a) **Adaptive Updating**: Continuously update the position of the evolved forecaster in the gene space as new instances arrive. (b) **Nearest Evolution**: If the instance surpasses the forecaster’s evolution threshold, evolve and replicate the closest forecaster at the instance. (c) **Optimizer Adjustment**: Adjust the learning rate for the shifted concept ■ to ensure accurate adaptation. (d) **Forecaster Elimination**: The forecaster f_4 associated with the rarely-occurring noise concept ■ may be removed due to prolonged inactivity. (e) **Nearest Retrieval**: Identify the nearest forecaster in the gene space when an input instance is encountered.

Data Format. A *univariate* time series is represented as $x = (x_1, x_2, \dots, x_N)$. Consider a look-back window of length L , which is denoted as $\mathbf{x}_i = (x_i, x_{i+1}, \dots, x_{i+L-1})$. The corresponding ground truth \mathbf{y}_i with a forecasting horizon of H is defined as $\mathbf{y}_i = (x_{i+L}, x_{i+L+1}, \dots, x_{i+L+H-1})$. Each pair of \mathbf{x}_i and \mathbf{y}_i forms an instance pair expressed as $\mathcal{D}_i = (\mathbf{x}_i, \mathbf{y}_i)$.

Problem Formulation. In contrast to traditional time series forecasting, online forecasting is partitioned into two distinct stages: (1) the warm-up stage and (2) the online stage. Once the dataset x is split into these two stages, sample pairs are constructed for each of them. The warm-up stage setting is consistent with

traditional time series forecasting. In the online stage, the step size of the instance pair is set as forecasting horizon in Figure 3. This setting effectively prevents the forecasting of the ground truth in the overlapping parts, which is in line with the setup of delayed feedback adopted in previous research Pham et al. (2023); Zhang et al. (2023). The batch size and epoch for the online stage are both set to 1. For *univariate time series without auxiliary information from other channels*, it is necessary to focus on the conceptual changes of the single channel itself. Previous research Zhang et al. (2023) has shown that time-channel independent online forecasting can reduce interference from too many channels.



Figure 3 Delayed feedback setting. The blue region represents the input, while the yellow region denotes the corresponding ground truth. In the previous online forecasting setting, the model knows part of the ground truth for the next sample beforehand. This situation is considered *unfair*. In the real world, the model must predict the future values of the ground truth. Therefore, a delay setting is used here.

3.1 Warm-Up Stage

Pool Initialization. We first initialize a pool set $Pl = \{(f(\theta_1), \mathbf{z}_1)\}$ with a single element. Here, $f(\theta_1)$ represents the initialized initial forecaster with parameter θ_1 , and \mathbf{z}_1 is the corresponding gene vector that stores the features of the instances. The gene, serving as a statistical signature for the underlying data distribution, is composed of two parts with a gene ratio τ_{gene} , as defined in Equation (3): the global gene vector \mathbf{z}_g and the local gene vector \mathbf{z}_l . The global gene \mathbf{z}_g is designed to capture and record long-term macroscopic features, which are crucial for forecasting. In contrast, the local gene \mathbf{z}_l is responsible for documenting short-term features that are strongly correlated with the current time. This design adopts a decoupled strategy: genes capture high-level regime shifts, ensuring the forecaster focuses on learning complex dependencies without being distracted by statistical noise. During the warm-up stage, which has the same task as typical time series forecasting, CEP employs the initial forecaster to make forecasts and accumulate knowledge for the online stage with recurring concepts.

$$\mathbf{z} = \tau_{gene} \cdot \mathbf{z}_l + (1 - \tau_{gene}) \cdot \mathbf{z}_g \quad (3)$$

Adaptive Updating. There are several necessary conditions for the gene implementation: **(1)** In the absence of historical samples, genes can be dynamically updated. **(2)** The distances between genes are statistically grounded. **(3)** Gene computation is highly efficient. Therefore, the gene of each instance \mathbf{x} is designed to use statistical moments in Equation (4), where μ is the mean operator, σ is the standard deviation operator, S limits the look-back window scope. This is a simple, yet effective approach, instead of considering more complex features such as spectral domain or periodic patterns. While spectral features could offer richer representations, this is hard to dynamically update under the previous conditions. The genes are adaptively updated as instances arrive, stabilizing over time in Figure 2(a).

Local genes are updated by Exponential Moving Average (EMA) with ratio τ_l for short-term adaptation in Equation (5), while global genes employ statistical formulas for overall trend estimation in Equation (6). EMA introduces an **implicit soft transition**, allowing the forecaster to smoothly track gradual drifts before a distinct concept split is triggered. The online update mechanism is derived in Appendix Section B.4.

$$\mathbf{z}_x = \text{Gene}(x) = (\mu(\mathbf{x}[-S :]), \sigma(\mathbf{x}[-S :])) \quad (4)$$

$$\mathbf{z}_l \leftarrow \tau_l \cdot \mathbf{z}_x + (1 - \tau_l) \cdot \mathbf{z}_l \quad (5)$$

$$\mathbf{z}_g \leftarrow \left(\frac{n \cdot \mathbf{z}_{g,\mu} + \mathbf{z}_{x,\mu}}{n + 1}, \sqrt{\frac{n}{n + 1} \mathbf{z}_{g,\sigma}^2 + \frac{n}{(n + 1)^2} (\mathbf{z}_{g,\mu} - \mathbf{z}_{x,\mu})^2} \right) \quad (6)$$

Additionally, *adaptive updating is not only limited to the warm-up stage but also applies to the online stage.* In the case of continuous concept drift shown in Section 4.2, the forecaster can adapt naively. This prevents the unnecessary evolution of additional forecasters, which would otherwise cause sample dispersion and hinder effective training. The updating behaviour can enable the forecaster to follow the slight and continuous changes in the data.

3.2 Online Stage

Nearest Retrieval. For a new instance \mathbf{x} with gene \mathbf{z}_x , the closest forecaster is retrieved using Euclidean distance (Equation (7), Equation (8)), with theoretical justification in Appendix Section B.2. We deliberately employ an assignment strategy to prevent Concept Interference, which refers to a phenomenon prevalent in soft-gating ensembles where irrelevant experts introduce noise during abrupt shifts. By activating only the most relevant forecaster, CEP enforces strict modularity, allowing each model to specialize in a distinct distribution without gradient pollution from conflicting concepts. To empirically validate this sparse activation choice against differentiable gating mechanisms such as MoE, we provide a detailed comparative analysis in Appendix C.6. We deliberately choose Euclidean distance instead of shape-based metrics such as Dynamic Time Warping to strictly adhere to privacy constraints where raw historical data cannot be retained, making gene-space retrieval a necessary proxy.

$$d(\mathbf{z}_x, \mathbf{z}) = \|\mathbf{z}_x - \mathbf{z}\|_2 \quad (7)$$

$$(f(\theta_N), \mathbf{z}_N) = \underset{(f(\theta_i), \mathbf{z}_i) \in Pl}{\operatorname{argmin}} d(\mathbf{z}_x, \mathbf{z}_i) \quad (8)$$

Nearest Evolution. Given that the instances in online time series forecasting arrive incrementally, the features of different concepts may exhibit instability during the initial stages. To ensure the stability of the gene, each forecaster in the pool Pl is assigned a safety period τ_{saf_e} . During the online phase, if the number of forecasting instances completed by $f(\theta_N)$ is fewer than the safety period, no splitting operation is executed. Conversely, when the number of completed forecasting instances by $f(\theta_N)$ reaches or exceeds the safety period, the splitting threshold τ_μ is determined. Once this threshold is exceeded, it implies that a distribution shift has occurred in the current instance. The threshold τ_μ in Equation (9) is established to detect the recurring concepts for the mean. If the threshold is surpassed, the evolution process, as described in Equation (10), is initiated. Upon evolution, a split forecaster is added to the evolution pool Pl . The newly created forecaster inherits the parameters of the nearest forecaster $f(\theta_N)$, and simultaneously, its corresponding gene inherits the gene g_x of the input instance, as shown in Figure 2(b). *This choice leverages transfer learning; by initializing from the closest existing model, the new forecaster starts with a strong inductive bias, significantly accelerating convergence on the new but related concept compared to initializing from scratch.*

$$|\mathbf{z}_{x,\mu} - \mathbf{z}_{N,\mu}| > \tau_\mu \cdot \mathbf{z}_{N,\sigma} \quad (9)$$

$$Pl \leftarrow Pl \cup \{(f(\theta_N), \mathbf{z}_x)\} \quad (10)$$

Detailed statistical justification is provided in Appendix Section B.3. Subsequently, the split forecaster will be tasked with forecasting the instance \mathbf{x} and updating its parameters. *It is important to note that in online forecasting, the normalization layer typically maintains the current concept. For CEP, the evolution mechanism serves a similar purpose.* On one hand, the evolution mechanism ensures that the samples learned by the forecasters in the pool belong to individual concepts. On the other hand, CEP does not focus on the internal design of the forecaster, aiming to enhance generalization and accommodate a wider range of forecasters.

Forecaster Elimination. Forecasters that remain idle for extended periods are removed to mitigate errors from time series fluctuations and conserve storage (Figure 2(d)). A threshold τ_e triggers elimination when $n_{wait} > \tau_e \cdot n_{pred}$ (Equation (11)), where n_{wait} is idle time which refers to the number of time points that have passed since the last prediction and n_{pred} is total predictions. This mechanism optimizes the system’s **active working memory** for edge deployment; removed concepts can theoretically be offloaded to hierarchical cold storage (e.g., disk) to handle long-term recurrence without consuming runtime resources. This mechanism promptly removes erroneously evolved forecasters and prevents noise corruption. Strategies such as the First-in-First-out (FIFO) method can be employed to control the maximum forecasters in the pool. The forecaster number variations of the forecasters in the processes of experiment are shown in the Appendix Figure 10.

$$n_{wait} > \tau_e \cdot n_{pred} \tag{11}$$

Optimizer Adjustment. For abrupt concept shifts (Figure 2(c)), the learning rate is adjusted as $lr = \tau_{lr} \cdot lr_{raw}$ initially, then gradually restored by exponential decay (Equation (12)), where t_{lr} is warming time. This balances rapid adaptation with stable convergence.

$$lr \leftarrow \max(lr_{raw}, \tau_{lr}^{-\frac{1}{t_{lr}}} \cdot lr) \tag{12}$$

Gradient Abandonment. If the ground truth gene \mathbf{g}_y triggers a split (Equation (9)), parameter updating is skipped to prevent concept contamination from anticipated distribution shifts, preserving forecaster specialization.

3.3 Hyperparameter Configuration

The thresholds in our user-driven algorithm are configurable, allowing performance to be tuned; for example, the mean threshold τ_μ in Equation (9) influences splitting frequency, with lower values promoting more aggressive divisions similar to temperature. This study employs empirically determined parameters. The choice of $\tau_\mu = 3$ is grounded in the Three-Sigma Rule of Empirical Statistics, rather than being an arbitrary heuristic. This effectively creates a 99.7% confidence interval for the current concept, ensuring that evolution is triggered only by statistically significant outliers. *This theoretical grounding allows CEP to be deployed across diverse domains without the need for extensive per-dataset hyperparameter tuning.* This facilitates a statistically grounded approach to identifying shifts warranting new forecaster evolution. At the same time, we conducted sensitivity tests for different thresholds to provide a reference for the performance of the CEP in Appendix Section C.8.

4 Experiments

4.1 Experiment Setting

Datasets. We evaluate CEP on a diverse array of real-world datasets. These datasets encompass: the ECL dataset [Trindade \(2015\)](#), the ETT dataset (comprising 4 distinct subsets) [Zhou et al. \(2021\)](#), the Exchange dataset [Wu et al. \(2021\)](#), the Traffic dataset [Wu et al. \(2021\)](#), and the WTH dataset [Wu et al. \(2021\)](#).

Baselines. In our experiments, we evaluated multiple baselines across the domains of continual learning, time series forecasting, and online learning. The Experience Replay (ER) method [Chaudhry et al. \(2019\)](#) stores historical data in a buffer and interleaves it with new samples during the learning process. DER++ [Buzzega](#)

et al. (2020) incorporates a knowledge distillation strategy to enhance performance. FSNet Pham et al. (2023) utilizes a fast-slow learning mechanism to capture both short-term changes and long-term patterns in online time series forecasting. OneNet Zhang et al. (2023) improves time series forecasting under concept drift through online ensembling, which combines multiple models to adapt to evolving data distributions and boost performance. For time series forecasting, we screened models based on various backbones, including: DLinear Zeng et al. (2023), TimesNet Wu et al. (2023), PatchTST Nie et al. (2023), SegRNN Lin et al. (2023), iTransformer Liu et al. (2024), and TimeMixer Wang et al. (2024). In all benchmarks, the length of the look-back window was set to $L = 60$, and the forecast horizon was varied as $H \in \{30, 60\}$. The metric used for evaluation was Mean Squared Error (MSE).

4.2 Main Results

4.2.1 Comparison with Base Forecasting Models

Experiment results are presented in Table 1. The proposed CEP generally reduces the MSE in forecasting across diverse datasets and model architectures. This reduction in MSE indicates that CEP effectively captures and utilizes the features of different concepts, thereby enhancing the performance of online time series forecasting in scenarios with recurring concept drift. CEP’s effectiveness is not limited to a single architecture or dataset, demonstrating its broad applicability. Notably, the TCN model Pham et al. (2023) experiences a particularly significant improvement in univariate online forecasting scenarios, with the MSE reduction exceeding 20%. This substantial improvement can be attributed to the unique characteristics of TCN, which leverages both time and variable dimensions in its design. In contrast, models like PatchTST Nie et al. (2023) rely solely on the time dimension, potentially limiting their ability to adapt to complex concept drifts. However, CEP may not yield improvements in specific cases, such as the Traffic dataset. We attribute this to the nature of its concept drifts. The Traffic dataset exhibits frequent, low-magnitude fluctuations rather than the distinct, recurring concepts CEP is designed to capture. Crucially, this result validates the robustness of CEP’s detection mechanism. In the Traffic dataset, which is dominated by micro-fluctuations rather than macro-distribution shifts, CEP correctly withheld unnecessary evolution. Unlike hyper-sensitive detectors that might trigger false alarms (and thus catastrophic forgetting), CEP preserves the stable macroscopic model, demonstrating its ability to distinguish signal from noise. This validates our decoupled adaptation hypothesis: for micro-fluctuations (like in Traffic) where macro-properties remain stable, the neural network’s gradient descent suffices, and CEP correctly avoids unnecessary intervention.

Table 1 The averaged MSE errors of different forecasters when using CEP are presented. Enhanced and reduced outcomes are marked with and respectively. The **best** and **second-best** performances are highlighted. The full results are presented in Appendix Table 8.

Data	TimeMixer	+CEP 	iTransformer	+CEP 	PatchTST	+CEP 	DLinear	+CEP 	SegRNN	+CEP 	TimesNet	+CEP 	TCN	+CEP
ECL	0.290	0.271	0.275	0.256	0.310	0.297	0.307	0.299	0.278	0.276	0.305	0.289	0.344	0.309
	-	-6.62%	-	-6.98%	-	-4.29%	-	-2.60%	-	-0.79%	-	-5.34%	-	-10.16%
ETTh1	0.335	0.322	0.326	0.323	0.332	0.327	0.337	0.308	0.303	0.301	0.351	0.341	0.463	0.459
	-	-3.91%	-	-0.80%	-	-1.75%	-	-8.70%	-	-0.76%	-	-2.96%	-	-0.76%
ETTh2	2.630	2.508	2.566	2.542	2.594	2.458	2.718	2.630	2.628	2.584	2.676	2.560	3.166	2.804
	-	-4.65%	-	-0.93%	-	-5.23%	-	-3.22%	-	-1.66%	-	-4.37%	-	-11.44%
ETTh1	0.755	0.737	0.760	0.740	0.759	0.721	0.849	0.752	0.719	0.716	0.837	0.793	0.981	0.801
	-	-2.39%	-	-2.64%	-	-5.00%	-	-11.53%	-	-0.32%	-	-5.21%	-	-18.40%
ETTh2	0.237	0.235	0.240	0.238	0.237	0.236	0.235	0.227	0.232	0.228	0.258	0.255	0.271	0.264
	-	-0.76%	-	-0.79%	-	-0.55%	-	-3.36%	-	-1.85%	-	-1.05%	-	-2.48%
Exchange	0.356	0.342	0.385	0.367	0.371	0.350	0.408	0.377	0.295	0.294	0.422	0.394	0.542	0.412
	-	-4.02%	-	-4.73%	-	-5.61%	-	-7.44%	-	-0.51%	-	-6.59%	-	-23.90%
Traffic	0.478	0.478	0.486	0.486	0.586	0.586	0.628	0.628	0.812	0.812	0.544	0.544	0.691	0.691
	-	0.00%	-	0.00%	-	0.00%	-	0.00%	-	0.00%	-	0.00%	-	0.00%
WTH	0.356	0.355	0.353	0.352	0.354	0.353	0.342	0.340	0.341	0.342	0.364	0.364	0.376	0.382
	-	-0.31%	-	-0.23%	-	-0.23%	-	-0.35%	-	0.21%	-	-0.25%	-	1.44%

4.2.2 Comparison with Online Forecasting Models

Experiment results are presented in Table 2. ER, DER++, FSNet, and OneNet did not yield satisfactory performance in delayed scenarios. Experience replay methods Chaudhry et al. (2019); Buzzega et al. (2020) reuse instances stored in memory to update the model. However, as time progresses, due to the limited memory capacity, the samples in memory may fail to retain the concepts that emerged earlier because of concept drift. FSNet Pham et al. (2023) is prone to forecasting biases, an inevitable consequence of the delayed arrival of samples. OneNet Zhang et al. (2023) takes short-term information into account to adjust model parameters, thus partially optimizing forecasting results in delayed scenarios. To preserve the knowledge of different concepts comprehensively, the proposed CEP employs a pooling mechanism to assign different concepts to distinct models. In delay-feedback scenarios, the performance achieved by CEP significantly outperforms that of previous state-of-the-art methods. This suggests that in delay scenarios, especially those with recurring concepts, previous online methods do not perform as effectively as anticipated and may even be inferior to the naive model shown in Table 2. In contrast, CEP can effectively manage recurring concepts. Furthermore, considering the rising prominence of generalist models, we extend our evaluation to compare CEP against latest TSFMs in zero-shot settings; detailed results regarding accuracy and resource efficiency are provided in Appendix C.7.

Table 2 The average MSE error of previous online forecasting methods. The previous methods all integrated TCN according to the original settings, and CEP’s forecaster is also TCN. Enhanced and reduced outcomes are marked with and respectively, the percentages represents the difference compared to TCN. The **best** and **second-best** performances are highlighted. Full results are presented in Appendix Table 9.

Data	ECL	ETTh1	ETTh2	ETTm1	ETTm2	Exchange	Traffic	WTH
TCN	<u>0.344</u>	0.463	3.166	<u>0.981</u>	<u>0.271</u>	<u>0.542</u>	<u>0.691</u>	0.376
ER	0.624 81.16%	0.454 -1.88%	3.329 5.16%	1.382 40.81%	0.322 19.06%	2.909 437.19%	1.110 60.60%	0.558 48.29%
DER++	0.580 68.26%	0.407 -12.12%	3.073 -2.94%	1.213 23.61%	0.304 12.38%	2.515 364.47%	1.076 55.67%	0.529 40.69%
FSNet	0.843 144.72%	0.470 1.51%	4.072 28.61%	1.562 59.17%	0.347 28.15%	3.486 543.77%	1.466 112.05%	0.743 97.53%
OneNet	0.425 23.49%	<u>0.410</u> -11.47%	3.402 7.47%	1.093 11.39%	0.285 5.10%	1.130 108.72%	0.673 -2.65%	0.414 10.12%
CEP 	0.309 -10.16%	0.459 -0.76%	2.804 -11.44%	0.801 -18.40%	0.264 -2.48%	0.412 -23.90%	<u>0.691</u> 0.00%	<u>0.382</u> 1.44%

4.3 Visualization

Figures 4 and 5 illustrate the forecasting results and MSE of both the naive model and the CEP. When the concept recurs (instances 2-14), the naive model exhibits a significant performance degradation, as evidenced by the surge in MSE. In contrast, CEP maintains a stable and low MSE, demonstrating its effective adaptation to the recurring concept. Figure 6 provides insight into the internal mechanism of CEP. The different colors represent distinct forecasters within the pool. The visualization confirms that CEP promptly activates a specialized forecaster (Forecaster 1) that has learned the features of the recurring concept. This targeted activation is the reason for its superior performance, as it avoids catastrophic forgetting and leverages stored knowledge.

4.4 Computational Complexity

In terms of time complexity, CEP is highly efficient. As it activates only a single specialized forecaster per instance, its inference time is nearly identical to that of the base forecaster model. **Regarding space complexity**, the *Forecaster Elimination* mechanism is crucial for preventing the unbounded growth of the forecaster pool. By dynamically pruning forecasters associated with outdated or transient concepts, this mechanism ensures the memory footprint remains practical and bounded. A more detailed analysis is provided in Appendix D.

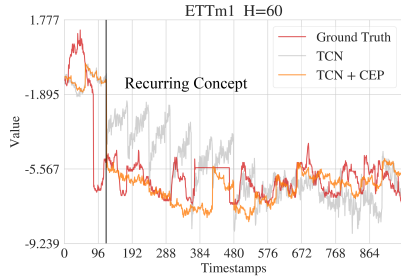


Figure 4 Visualization of forecasting results

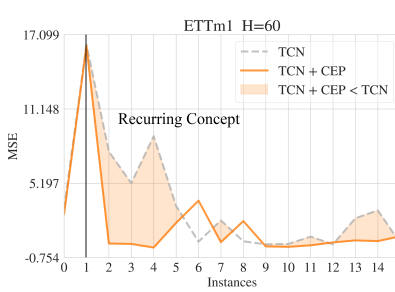


Figure 5 Visualization of Metric

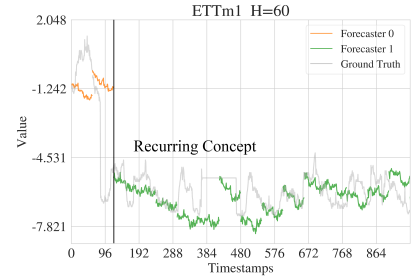


Figure 6 Visualization of different forecaster results in CEP

4.5 Model Analysis

To validate the efficacy of each component in CEP, we conducted extensive ablation studies, with the results presented in Table 3. One of the key findings is that the evolutionary mechanism is indispensable; for instance, disabling Evolution for the TCN forecaster leads to a substantial increase in prediction error, demonstrating that our evolutionary framework is crucial for performance. The complete CEP yielded the best results, significantly outperforming all ablated versions. Interestingly, the second-best performance was achieved without the Elimination mechanism. This highlights the dual role of elimination: it not only maintains a manageable pool size but also discards outdated knowledge, ensuring the model’s continuous adaptation. Comprehensive ablation results and other experimental details, including sensitivity, are provided in Appendix C.

Table 3 The MSE error of the ablation experiments with forecaster TCN. The results are the mean values of different backbone forecasters. The **best** and **second-best** performances are highlighted. Full results are presented in Appendix Table 10.

Dataset		ECL	ETTh1	ETTh2	ETTm1	ETTm2	Exchange	Traffic	WTH	AVG
CEP		0.314	<u>0.438</u>	<u>2.799</u>	0.801	<u>0.256</u>	<u>0.404</u>	0.710	0.379	0.762
Base TCN (<i>w/o</i> Evolution)		0.347	0.436	3.106	0.991	0.261	0.524	0.710	0.375	0.844
<i>w/o</i> Local Gene		<u>0.317</u>	0.451	2.904	0.801	0.257	0.524	0.710	<u>0.375</u>	0.792
<i>w/o</i> Global Gene		0.321	<u>0.438</u>	2.872	0.865	<u>0.256</u>	0.401	0.710	0.367	0.779
<i>w/o</i> Elimination		0.335	<u>0.438</u>	2.797	0.801	0.254	0.406	0.710	0.379	<u>0.765</u>

5 Conclusion

In this paper, we address the critical challenge of recurring concept drift in online time series forecasting, where models often suffer from catastrophic forgetting. We introduce CEP, an evolutionary framework that maintains a diverse pool of specialized forecasters to preserve learned concepts. By evolving new forecasters from the most relevant existing ones and eliminating outdated knowledge, CEP effectively adapts to concept shifts. Our experiments demonstrate that CEP significantly enhances long-horizon forecasting performance, overcoming the limitations of current online methods that struggle with knowledge retention. Future work will explore richer gene representations, potentially incorporating higher-order moments or spectral features to address more complex drifts, and extend this framework to handle asynchronous shifts in multivariate time series.

References

- Cesare Alippi, Giacomo Boracchi, and Manuel Roveri. Just-in-time classifiers for recurrent concepts. *IEEE transactions on neural networks and learning systems*, 24(4):620–634, 2013.
- Abdul Fatir Ansari, Lorenzo Stella, Caner Turkmen, Xiyuan Zhang, Pedro Mercado, Huibin Shen, Oleksandr Shchur, Syama Sundar Rangapuram, Sebastian Pineda Arango, Shubham Kapoor, et al. Chronos: Learning the language of time series. *arXiv preprint arXiv:2403.07815*, 2024.
- Albert Bifet and Ricard Gavaldà. Adaptive learning from evolving data streams. In *International symposium on intelligent data analysis*, pages 249–260. Springer, 2009.
- Pietro Buzzega, Matteo Boschini, Angelo Porrello, Davide Abati, and Simone Calderara. Dark experience for general continual learning: a strong, simple baseline. *Advances in neural information processing systems*, 33:15920–15930, 2020.
- Arslan Chaudhry, Marcus Rohrbach, Mohamed Elhoseiny, Thalaiyasingam Ajanthan, Puneet K. Dokania, Philip H. S. Torr, and Marc’Aurelio Ranzato. On tiny episodic memories in continual learning, 2019.
- Abhimanyu Das, Weihao Kong, Rajat Sen, and Yichen Zhou. A decoder-only foundation model for time-series forecasting. In *Forty-first International Conference on Machine Learning*, 2024.
- Gregory Ditzler, Manuel Roveri, Cesare Alippi, and Robi Polikar. Learning in nonstationary environments: A survey. *IEEE Computational intelligence magazine*, 10(4):12–25, 2015.
- Yuntao Du, Jindong Wang, Wenjie Feng, Sinno Pan, Tao Qin, Renjun Xu, and Chongjun Wang. Adarnn: Adaptive learning and forecasting of time series. In *Proceedings of the 30th ACM International Conference on Information & Knowledge Management*, 2021.
- Ryan Elwell and Robi Polikar. Incremental learning of concept drift in nonstationary environments. *IEEE transactions on neural networks*, 22(10):1517–1531, 2011.
- Heitor M Gomes, Albert Bifet, Jesse Read, Jean Paul Barddal, Fabrício Enembreck, Bernhard Pfharinger, Geoff Holmes, and Talel Abdesslem. Adaptive random forests for evolving data stream classification. *Machine Learning*, 106(9):1469–1495, 2017.
- Elad Hazan et al. Introduction to online convex optimization. *Foundations and Trends® in Optimization*, 2(3-4): 157–325, 2016.
- Ferenc Huszár. Note on the quadratic penalties in elastic weight consolidation. *Proceedings of the National Academy of Sciences*, 115(11):E2496–E2497, 2018.
- Sheo Yon Jhin, Seojin Kim, and Noseong Park. Addressing prediction delays in time series forecasting: A continuous gru approach with derivative regularization. In *Proceedings of the 30th ACM SIGKDD Conference on Knowledge Discovery and Data Mining*, pages 1234–1245, 2024.
- Ming Jin, Huan Yee Koh, Qingsong Wen, Daniele Zambon, Cesare Alippi, Geoffrey I Webb, Irwin King, and Shirui Pan. A survey on graph neural networks for time series: Forecasting, classification, imputation, and anomaly detection. *IEEE Transactions on Pattern Analysis and Machine Intelligence*, 2024.
- Nicolas Johansson, Tobias Olsson, Daniel Nilsson, Johan Östman, and Fazeleh Hoseini. Privacy risks in time series forecasting: User-and record-level membership inference. *arXiv preprint arXiv:2509.04169*, 2025.
- Minsu Kim, Seong-Hyeon Hwang, and Steven Euijong Whang. Quilt: robust data segment selection against concept drifts. In *Proceedings of the AAAI Conference on Artificial Intelligence*, volume 38, pages 21249–21257, 2024.
- Taesung Kim, Jinhee Kim, Yunwon Tae, Cheonbok Park, Jang-Ho Choi, and Jaegul Choo. Reversible instance normalization for accurate time-series forecasting against distribution shift. In *International Conference on Learning Representations*, 2022.
- James Kirkpatrick, Razvan Pascanu, Neil Rabinowitz, Joel Veness, Guillaume Desjardins, Andrei A Rusu, Kieran Milan, John Quan, Tiago Ramalho, Agnieszka Grabska-Barwinska, et al. Reply to huszár: The elastic weight consolidation penalty is empirically valid. *Proceedings of the National Academy of Sciences*, 115(11):E2498–E2498, 2018.
- Shengsheng Lin, Weiwei Lin, Wentai Wu, Feiyu Zhao, Ruichao Mo, and Haotong Zhang. Segrnn: Segment recurrent neural network for long-term time series forecasting, 2023.

- Yong Liu, Tengge Hu, Haoran Zhang, Haixu Wu, Shiyu Wang, Lintao Ma, and Mingsheng Long. itransformer: Inverted transformers are effective for time series forecasting. In *The Twelfth International Conference on Learning Representations*, 2024.
- Yuqi Nie, Nam H Nguyen, Phanwadee Sinthong, and Jayant Kalagnanam. A time series is worth 64 words: Long-term forecasting with transformers. In *The Eleventh International Conference on Learning Representations*, 2023.
- Quang Pham, Chenghao Liu, Doyen Sahoo, and Steven Hoi. Learning fast and slow for online time series forecasting. In *The Eleventh International Conference on Learning Representations*, 2023.
- Jesse Read. Concept-drifting data streams are time series; the case for continuous adaptation. *arXiv preprint arXiv:1810.02266*, 2018.
- Noam Shazeer, Azalia Mirhoseini, Krzysztof Maziarczyk, Andy Davis, Quoc Le, Geoffrey Hinton, and Jeff Dean. Outrageously large neural networks: The sparsely-gated mixture-of-experts layer. In *International Conference on Learning Representations*, 2017.
- Artur Trindade. ElectricityLoadDiagrams20112014. UCI Machine Learning Repository, 2015.
- Alexey Tsymbal. The problem of concept drift: definitions and related work. *Computer Science Department, Trinity College Dublin*, 106(2):58, 2004.
- Ke Wan, Yi Liang, and Susik Yoon. Online drift detection with maximum concept discrepancy. In *Proceedings of the 30th ACM SIGKDD Conference on Knowledge Discovery and Data Mining*, page 2924–2935, 2024.
- Shiyu Wang, Haixu Wu, Xiaoming Shi, Tengge Hu, Huakun Luo, Lintao Ma, James Y. Zhang, and JUN ZHOU. Timemixer: Decomposable multiscale mixing for time series forecasting. In *The Twelfth International Conference on Learning Representations*, 2024.
- Barry Payne Welford. Note on a method for calculating corrected sums of squares and products. *Technometrics*, 4(3): 419–420, 1962.
- Gerald Woo, Chenghao Liu, Akshat Kumar, Caiming Xiong, Silvio Savarese, and Doyen Sahoo. Unified training of universal time series forecasting transformers. In *International Conference on Machine Learning*, pages 53140–53164. PMLR, 2024.
- Haixu Wu, Jiehui Xu, Jianmin Wang, and Mingsheng Long. Autoformer: decomposition transformers with auto-correlation for long-term series forecasting. In *Proceedings of the 35th International Conference on Neural Information Processing Systems*, 2021.
- Haixu Wu, Tengge Hu, Yong Liu, Hang Zhou, Jianmin Wang, and Mingsheng Long. Timesnet: Temporal 2d-variation modeling for general time series analysis. In *The Eleventh International Conference on Learning Representations*, 2023.
- Ailing Zeng, Muxi Chen, Lei Zhang, and Qiang Xu. Are transformers effective for time series forecasting? *Proceedings of the AAAI Conference on Artificial Intelligence*, 37(9):11121–11128, 2023.
- Yifan Zhang, Qingsong Wen, xue wang, Weiqi Chen, Liang Sun, Zhang Zhang, Liang Wang, Rong Jin, and Tieniu Tan. Onenet: Enhancing time series forecasting models under concept drift by online ensembling. In *Advances in Neural Information Processing Systems*, 2023.
- Haoyi Zhou, Shanghang Zhang, Jieqi Peng, Shuai Zhang, Jianxin Li, Hui Xiong, and Wancai Zhang. Informer: Beyond efficient transformer for long sequence time-series forecasting. In *Proceedings of the AAAI conference on artificial intelligence*, volume 35, pages 11106–11115, 2021.
- Martin Zinkevich. Online convex programming and generalized infinitesimal gradient ascent. In *Proceedings of the 20th international conference on machine learning (icml-03)*, pages 928–936, 2003.

Appendix Table of Contents

A	Notations	13
B	Technical Details	13
B.1	Algorithm Motivation	13
B.2	Statistical Foundation of Gene Representation	14
B.3	Design Rationale of Gene Representation	16
B.4	Derivation of Online Gene Update	17
B.5	Regret Decomposition Analysis	19
C	Experiment Details	19
C.1	Dataset	19
C.2	Experimental Setting	20
C.3	Full Experiment Result of Base Forecasters	20
C.4	Full Experiment Result of Online Methods	22
C.5	Ablation Study	22
C.6	Full Experiment Result of Forecaster Assignment Mechanisms	24
C.7	Full Experiment Result of Time Series Foundation Models	25
C.8	Hyperparameter Sensitivity	25
C.9	Practical Usage Guide	27
D	Complexity Analysis	28

A Notations

In this section, we provide a summary of the notation used in the main paper, particularly in the method section, for quick reference. Table 4 lists the key symbols and their corresponding descriptions.

B Technical Details

B.1 Algorithm Motivation

The core principle of the Continuous Evolution Pool (CEP) is to partition the online data stream into distinct concepts and dedicate a specialized forecaster to each. This approach directly tackles catastrophic forgetting by isolating the learning process for each concept, preventing knowledge from one from being overwritten by another. It contrasts with standard online learning, where a single model continuously adapts, and with Experience Replay Chaudhry et al. (2019), where stored samples may become outdated or fail to represent all past concepts.

Conceptually, CEP operationalizes the ideal of partitioning a dataset \mathcal{D} into subsets $\tilde{\mathcal{D}}_i$, where each subset contains instances from a single data distribution p_i . In an online setting, this partitioning must be performed dynamically without storing past instances due to privacy or memory constraints. CEP achieves this by using a statistical gene to identify the concept of each incoming instance \mathcal{D}_i . It then assigns the instance to the forecaster with the most similar gene, ensuring that each forecaster is trained only on data from its designated

Table 4 Summary of important notations.

Notation	Description	Hyperparameter
p	Probability distribution of time series	
x	Original time series	
\mathbf{x}_i	Input window	
\mathbf{y}_i	Ground truth window	
\mathbf{L}	Input window length	
\mathbf{H}	Forecasting horizon	
C_i	Concept i	
\mathcal{D}_i	Input and ground truth window pair: Data pair	
\mathcal{D}	Data pairs	
$\tilde{\mathcal{D}}_i$	Data pairs of concept i	
Pl	Forecaster Pool	
$f(\cdot)$	Forecaster	
θ_i	Forecaster parameter of concept i	\times
\mathbf{z}_i	Gene of concept i	
\mathbf{z}_l	Local gene	
\mathbf{z}_g	Global gene	
\mathbf{z}_x	Sample gene	
μ	Mean	
σ	Standard deviation	
S	Scope of μ and σ	
n	Number of historical samples	
$d(\cdot, \cdot)$	Distance of gene	
N	Nearest neighbor	
n_{wait}	Number of wait time of forecaster	
n_{pred}	Number of prediction of forecaster	
lr	Learning rate	
τ_{gene}	Global gene ratio	
τ_l	local Gene ratio	
τ_μ	Mean threshold for splitting	
τ_{safe}	Initialization time of forecaster	\checkmark
τ_e	Elimination threshold of forecaster	
τ_{lr}	Adjustment ratio of learning rate	

concept. This process effectively handles the challenges of online learning, such as imbalanced data and the non-sequential arrival of concepts, by promptly selecting an appropriate, pre-specialized model. The complete workflow is presented in Algorithm ??.

B.2 Statistical Foundation of Gene Representation

In the context of online time series forecasting, we contend that complex representations such as spectral features (e.g., Fourier coefficients) or shapelets are unnecessary and computationally prohibitive. Instead, the first two statistical moments (mean and variance) constitute the *minimal sufficient statistics* required to satisfy the three critical constraints inherent to the problem setting:

1. **Dynamic Updatability.** In strictly privacy-preserving or memory-constrained online settings, historical raw samples cannot be retained. Consequently, the feature representation must support incremental updates with $O(1)$ time and space complexity. Mean and variance strictly satisfy this requirement by online algorithm [Welford \(1962\)](#), the detailed derivation of which is provided in [Appendix B.4](#). This allows the global gene to evolve continuously as new data arrives without accessing past samples. In contrast, frequency-domain features such as FFT or shape-based methods typically require buffering entire windows or historical subsequences to compute similarity, which violates the memory-less constraint and complicates incremental updates.

Algorithm 1: Continuous Evolution Pool

Initialize

```
Dataset  $x$  ;  
Forecaster  $f$  ;  
 $\mathcal{D}_{warm}, \mathcal{D}_{online} \leftarrow \text{split}(x)$  ; ▷ Problem Formulation  
Initialize  $Pl = \{(f(\theta_1), \mathbf{z}_1)\}$  ;
```

Stage Warm-up

```
for  $\mathcal{D}_i \in \mathcal{D}_{warm}$  ; ▷  $\mathcal{D}_i = (\mathbf{x}_i, \mathbf{y}_i)$   
do  
   $\mathbf{z}_x = \text{Gene}(\mathbf{x}_i)$  ; ▷ Equation (4)  
   $\mathcal{L} = \text{Loss}(f(\mathbf{x}_i, \theta_1), \mathbf{y}_i)$  ;  
   $\theta_1 \leftarrow \theta_1 - lr * \nabla \mathcal{L}$  ;  
   $\mathbf{z}_1 \leftarrow \text{Update}(\mathbf{z}_1, \mathbf{z}_x)$  ; ▷ Update gene, Equation (3), Equation (5), Equation (6)
```

Stage Online

```
for  $\mathcal{D}_i \in \mathcal{D}_{online}$  ; ▷  $\mathcal{D}_i = (\mathbf{x}_i, \mathbf{y}_i)$   
do  
   $\mathbf{z}_x = \text{Gene}(\mathbf{x}_i)$  ; ▷ Equation (4)  
   $(f(\theta_n), \mathbf{z}_n) = \text{Nearest}(Pl, \mathbf{z}_x)$  ; ▷ Equation (7), Equation (8)  
  if  $\text{Evolution}(\mathbf{z}_x, \mathbf{z}_n)$  ; ▷ Evolve or retrieve, Equation (9)  
  then  
     $\theta_c = \text{Copy}(\theta_n)$  ; ▷ Evolve  
     $Pl \leftarrow Pl \cup (f(\theta_c), \mathbf{z}_x)$  ;  
     $lr \leftarrow \text{Adjust}(lr)$  ; ▷ Adjust optimizer, Equation (12)  
  else ▷ Retrieve  
     $\theta_c = \theta_n$  ;  
     $\hat{\mathbf{y}}_i = f(\mathbf{x}_i, \theta_c)$  ;  
     $\mathbf{z}_y = \text{Gene}(\mathbf{y}_i)$  ; ▷ Equation (4)  
    if not  $\text{Evolution}(\mathbf{z}_y, \mathbf{z}_n)$  ; ▷ Give up the polluted gradient, Equation (9)  
    then  
       $\mathcal{L} = \text{Loss}(\hat{\mathbf{y}}_i, \mathbf{y}_i)$  ;  
       $\theta_c \leftarrow \theta_c - lr * \nabla \mathcal{L}$  ;  
       $\mathbf{z}_c \leftarrow \text{Update}(\mathbf{z}_c, \mathbf{z}_x)$  ; ▷ Update gene, Equation (3), Equation (5), Equation (6)  
     $Pl \leftarrow \text{Eliminate}(Pl)$  ; ▷ Eliminate ineffective forecasters, Equation (11)
```

2. **Statistical Support for Drift Detection.** Since concept drift is fundamentally a shift in the joint probability distribution $p_t(\mathbf{x}, \mathbf{y})$, a rigorous distance metric is required to quantify this shift. The first two moments serve as foundational descriptors of the distribution; a significant divergence in sample mean or variance provides a direct, statistically grounded signal that $p_{t_1}(\mathbf{x}) \neq p_{t_2}(\mathbf{x})$. This interpretability allows us to employ standard hypothesis testing, specifically the Z-test used in our Evolution mechanism to define rigorous confidence intervals for drift detection. Conversely, latent representations from deep neural networks are often uninterpretable. Measuring drift in a high-dimensional latent space lacks a clear statistical threshold, making the definition of a drift distance arbitrary and sensitive to hyperparameter tuning.
3. **Computational Efficiency.** For deployment on edge devices with limited resources, the overhead of computing the gene must be negligible compared to the forecasting model itself. Computing moments involves only basic linear operations, ensuring minimal latency. Complex feature extraction methods, such as spectral analysis or deep embedding generation, add significant computational overhead that risks bottlenecking real-time inference pipelines.

Theoretical Derivation by Maximum Likelihood Estimation (MLE). Given that the mean and variance satisfy the above constraints, we further justify the use of Euclidean distance in the gene space through Maximum Likelihood Estimation. Assume that each learned concept C_k in the pool follows a stable Gaussian distribution $\mathcal{N}(\mu_k, \sigma_k^2)$. For a newly arrived input window $\mathbf{x} = \{x_1, \dots, x_L\}$, we aim to identify the concept k that maximizes the probability of generating \mathbf{x} . The likelihood function is:

$$p(\mathbf{x}|C_k) = \prod_{i=1}^L \frac{1}{\sqrt{2\pi\sigma_k^2}} \exp\left(-\frac{(x_i - \mu_k)^2}{2\sigma_k^2}\right) \quad (13)$$

Taking the logarithm to obtain the log-likelihood:

$$\log p(\mathbf{x}|C_k) = \sum_{i=1}^L \left[-\frac{1}{2} \log(2\pi) - \log(\sigma_k) - \frac{(x_i - \mu_k)^2}{2\sigma_k^2} \right] \quad (14)$$

ignoring the constant term $-\frac{L}{2} \log(2\pi)$, we maximize:

$$\mathcal{L}(\mathbf{x}|C_k) \propto -L \log(\sigma_k) - \frac{1}{2\sigma_k^2} \sum_{i=1}^L (x_i - \mu_k)^2 \quad (15)$$

To relate this to the sample statistics, we decompose the summation term $\sum_{i=1}^L (x_i - \mu_k)^2$. Let $\hat{\mu}_{\mathbf{x}} = \frac{1}{L} \sum_{i=1}^L x_i$ be the sample mean. We add and subtract $\hat{\mu}_{\mathbf{x}}$:

$$\sum_{i=1}^L (x_i - \mu_k)^2 = \sum_{i=1}^L ((x_i - \hat{\mu}_{\mathbf{x}}) + (\hat{\mu}_{\mathbf{x}} - \mu_k))^2 \quad (16)$$

Expanding the square:

$$= \sum_{i=1}^L (x_i - \hat{\mu}_{\mathbf{x}})^2 + \sum_{i=1}^L (\hat{\mu}_{\mathbf{x}} - \mu_k)^2 + 2(\hat{\mu}_{\mathbf{x}} - \mu_k) \underbrace{\sum_{i=1}^L (x_i - \hat{\mu}_{\mathbf{x}})}_0 \quad (17)$$

The cross-term is zero because $\sum (x_i - \hat{\mu}_{\mathbf{x}}) = \sum x_i - L \cdot \frac{1}{L} \sum x_i = 0$. Using the definition of sample variance $\hat{\sigma}_{\mathbf{x}}^2 = \frac{1}{L} \sum (x_i - \hat{\mu}_{\mathbf{x}})^2$, the equation simplifies to:

$$\sum_{i=1}^L (x_i - \mu_k)^2 = L\hat{\sigma}_{\mathbf{x}}^2 + L(\hat{\mu}_{\mathbf{x}} - \mu_k)^2 \quad (18)$$

Substituting this back into the objective function, maximizing the likelihood is equivalent to minimizing the negative log-likelihood cost function $J(k)$:

$$J(k) = 2 \log(\sigma_k) + \frac{\hat{\sigma}_{\mathbf{x}}^2}{\sigma_k^2} + \frac{(\hat{\mu}_{\mathbf{x}} - \mu_k)^2}{\sigma_k^2} \quad (19)$$

This derivation explicitly shows that the optimal concept selection depends on minimizing the difference between the sample statistics $(\hat{\mu}_{\mathbf{x}}, \hat{\sigma}_{\mathbf{x}})$ and the concept parameters (μ_k, σ_k) . The Euclidean distance used in CEP acts as a computationally efficient proxy for this statistically optimal objective.

B.3 Design Rationale of Gene Representation

Building upon the statistical validity of the gene, CEP employs specific mechanisms for drift detection and model assignment. These choices are designed to overcome the limitations of traditional ensemble methods in handling recurring concepts.

Evolution: Proactive Statistical Hypothesis Testing. Traditional drift detection methods often rely on monitoring prediction error such as ADWIN. These methods are inherently *reactive*: the model must experience a performance degradation with high error before the drift is detected. This lag is detrimental in time series forecasting, especially with delayed feedback. In contrast, CEP employs a *proactive* detection mechanism based on statistical hypothesis testing. We formulate the detection as:

- **Null Hypothesis (H_0):** The incoming sample \mathbf{x} is drawn from the distribution of the current concept C_N , i.e., $\mathbf{x} \sim \mathcal{N}(\mu_N, \sigma_N^2)$.
- **Test Statistic:** We reject H_0 if the sample mean deviates significantly from the concept mean, normalized by the concept’s standard deviation:

$$\frac{|\hat{\mu}_{\mathbf{x}} - \mu_N|}{\sigma_N} > \tau_\mu \quad (20)$$

By setting τ_μ based on standard confidence intervals ($\tau_\mu = 3$ corresponds to a 99.7% confidence interval), we can detect distribution shifts immediately upon data arrival, decoupling drift detection from forecasting error.

Assignment: Sparse Activation with Implicit Smoothing. While traditional ensemble methods such as OneNet rely on *explicit* soft weighting to smooth predictions, CEP adopts a strategy of **Sparse Activation with Implicit Smoothing**. This design leverages the continuous evolution of the gene by EMA to achieve stability, while employing decisive retrieval to maintain model purity.

1. **Implicit Continuity by Gene Trajectory.** Explicit soft-weighting methods smooth the output by averaging predictions, which often leads to prediction inertia where obsolete models drag down performance during abrupt shifts. In contrast, CEP achieves smoothing in the *concept space* rather than the *output space*. Since the local gene is updated by EMA in Equation (6), the forecaster’s representation moves along a continuous trajectory, shown in Fig.10. This allows the system to smoothly track gradual drifts and filter out high-frequency noise without the lag caused by averaging historical model outputs. The softness is implicit in the gene’s evolution, ensuring stability before a discrete switch occurs.
2. **Parameter Isolation by Sparse Activation.** Although the gene evolves smoothly, the assignment of the forecasting model remains *sparse* which means activating only the top-1 nearest neighbor. This creates a strict boundary that solves the gradient pollution problem inherent in soft ensembles. In a fully soft ensemble, backpropagation affects all models with non-zero weights, causing the current data to overwrite the parameters of experts specialized in latent or inactive concepts. By enforcing sparse activation, CEP structurally isolates the parameters of inactive forecasters, ensuring their specialized knowledge remains frozen and intact for future recurrence.

B.4 Derivation of Online Gene Update

Equation (6) provides an efficient online method to update the global gene $\mathbf{z}_g = (\mathbf{z}_{g,\mu}, \mathbf{z}_{g,\sigma})$, which represents the running mean and standard deviation of all instance genes encountered by a forecaster so far. This approach avoids storing all past data, making it highly suitable for online scenarios. Here, we provide a step-by-step derivation of these standard online update formulas.

Mean Update Derivation. Let $\mathbf{z}_{g,\mu,n}$ be the mean of the first n instance gene means, $\{\mathbf{z}_{x,\mu}^{(1)}, \mathbf{z}_{x,\mu}^{(2)}, \dots, \mathbf{z}_{x,\mu}^{(n)}\}$. By definition:

$$\mathbf{z}_{g,\mu,n} = \frac{1}{n} \sum_{i=1}^n \mathbf{z}_{x,\mu}^{(i)} \quad (21)$$

When a new instance gene with mean $\mathbf{z}_{x,\mu}^{(n+1)}$ arrives, the new global mean $\mathbf{z}_{g,\mu,n+1}$ is calculated as:

$$\mathbf{z}_{g,\mu,n+1} = \frac{1}{n+1} \sum_{i=1}^{n+1} \mathbf{z}_{x,\mu}^{(i)} \quad (22)$$

$$= \frac{1}{n+1} \left(\left(\sum_{i=1}^n \mathbf{z}_{x,\mu}^{(i)} \right) + \mathbf{z}_{x,\mu}^{(n+1)} \right) \quad (23)$$

$$= \frac{1}{n+1} \left(n \cdot \left(\frac{1}{n} \sum_{i=1}^n \mathbf{z}_{x,\mu}^{(i)} \right) + \mathbf{z}_{x,\mu}^{(n+1)} \right) \quad (24)$$

$$= \frac{n \cdot \mathbf{z}_{g,\mu,n} + \mathbf{z}_{x,\mu}^{(n+1)}}{n+1} \quad (25)$$

This recursive formula allows us to compute the new mean using only the previous mean, the new value, and the sample count n . This corresponds to the first component of Equation (6).

Variance Update Derivation. The variance update is derived using a similar recursive approach, often known as a form of Welford's algorithm. Let $\mathbf{z}_{g,\sigma,n}^2$ be the variance of the first n instance gene means. Let $M_{1,n} = \mathbf{z}_{g,\mu,n}$ be the first raw moment (the mean), and $M_{2,n} = \frac{1}{n} \sum_{i=1}^n (\mathbf{z}_{x,\mu}^{(i)})^2$ be the second raw moment. The variance is given by $\mathbf{z}_{g,\sigma,n}^2 = M_{2,n} - M_{1,n}^2$.

The moments can be updated online:

$$M_{1,n+1} = \frac{n \cdot M_{1,n} + \mathbf{z}_{x,\mu}^{(n+1)}}{n+1} \quad (26)$$

$$M_{2,n+1} = \frac{n \cdot M_{2,n} + (\mathbf{z}_{x,\mu}^{(n+1)})^2}{n+1} \quad (27)$$

Now, we derive the recursive formula for the variance $\mathbf{z}_{g,\sigma,n+1}^2$:

$$\mathbf{z}_{g,\sigma,n+1}^2 = M_{2,n+1} - M_{1,n+1}^2 \quad (28)$$

$$= \frac{nM_{2,n} + (\mathbf{z}_{x,\mu}^{(n+1)})^2}{n+1} - \left(\frac{nM_{1,n} + \mathbf{z}_{x,\mu}^{(n+1)}}{n+1} \right)^2 \quad (29)$$

$$= \frac{(n+1)(nM_{2,n} + (\mathbf{z}_{x,\mu}^{(n+1)})^2) - (n^2M_{1,n}^2 + 2nM_{1,n}\mathbf{z}_{x,\mu}^{(n+1)} + (\mathbf{z}_{x,\mu}^{(n+1)})^2)}{(n+1)^2} \quad (30)$$

Substituting $M_{2,n} = \mathbf{z}_{g,\sigma,n}^2 + M_{1,n}^2$ into the expression:

$$= \frac{n(n+1)(\mathbf{z}_{g,\sigma,n}^2 + M_{1,n}^2) + n(\mathbf{z}_{x,\mu}^{(n+1)})^2 - n^2M_{1,n}^2 - 2nM_{1,n}\mathbf{z}_{x,\mu}^{(n+1)}}{(n+1)^2} \quad (31)$$

$$= \frac{n(n+1)\mathbf{z}_{g,\sigma,n}^2 + (n^2+n)M_{1,n}^2 - n^2M_{1,n}^2 + n(\mathbf{z}_{x,\mu}^{(n+1)})^2 - 2nM_{1,n}\mathbf{z}_{x,\mu}^{(n+1)}}{(n+1)^2} \quad (32)$$

$$= \frac{n(n+1)\mathbf{z}_{g,\sigma,n}^2 + nM_{1,n}^2 - 2nM_{1,n}\mathbf{z}_{x,\mu}^{(n+1)} + n(\mathbf{z}_{x,\mu}^{(n+1)})^2}{(n+1)^2} \quad (33)$$

$$= \frac{n(n+1)\mathbf{z}_{g,\sigma,n}^2 + n(M_{1,n} - \mathbf{z}_{x,\mu}^{(n+1)})^2}{(n+1)^2} \quad (34)$$

$$= \frac{n}{n+1} \mathbf{z}_{g,\sigma,n}^2 + \frac{n}{(n+1)^2} (\mathbf{z}_{g,\mu,n} - \mathbf{z}_{x,\mu}^{(n+1)})^2 \quad (35)$$

This expression is a numerically stable and efficient way to update the variance. This ensures that the global gene accurately reflects the statistical properties of all data seen by its corresponding forecaster.

B.5 Regret Decomposition Analysis

We provide a regret decomposition analysis to illustrate the theoretical motivation behind CEP. Under the simplified assumption of locally stationary regimes, we provide a high-level regret analysis. Traditional regret compares an online algorithm’s cumulative loss to that of the best single fixed model in hindsight. However, this benchmark is ill-suited for concept drift scenarios, as no single model can perform optimally across all concepts. A more meaningful benchmark is an *oracle* that knows the true underlying concept at each time step and uses the optimal specialized forecaster for that concept.

Problem Formulation. Let the set of distinct, underlying concepts be $\mathcal{C} = \{C_1, \dots, C_K\}$, where each concept C_k is associated with a stationary data distribution $p_k(\mathbf{x}, \mathbf{y})$. For each concept C_k , there exists an optimal forecaster, $f_k^* = \arg \min_f \mathbb{E}_{(\mathbf{x}, \mathbf{y}) \sim p_k} [\mathcal{L}(f(\mathbf{x}), \mathbf{y})]$. At each time step t , the incoming data $(\mathbf{x}_t, \mathbf{y}_t)$ is generated from a distribution corresponding to the active concept $C(t) \in \mathcal{C}$. The oracle’s cumulative loss over a horizon T is $\sum_{t=1}^T \mathcal{L}_t(f_{C(t)}^*)$.

The regret of CEP, R_T^{CEP} , is the difference between its cumulative loss and the oracle’s:

$$R_T^{\text{CEP}} = \sum_{t=1}^T \mathcal{L}_t(f_{\text{sel}}(t)) - \sum_{t=1}^T \mathcal{L}_t(f_{C(t)}^*) \quad (36)$$

where $f_{\text{sel}}(t)$ is the forecaster selected by CEP at time t .

Decomposition of Regret. The total regret can be decomposed into two primary components. Let $f_{\text{CEP}}(t)$ be the forecaster within CEP’s pool that is designated for the true concept $C(t)$.

$$R_T^{\text{CEP}} = \underbrace{\sum_{t=1}^T (\mathcal{L}_t(f_{\text{sel}}(t)) - \mathcal{L}_t(f_{\text{CEP}}(t)))}_{\text{Identification Regret}} + \underbrace{\sum_{t=1}^T (\mathcal{L}_t(f_{\text{CEP}}(t)) - \mathcal{L}_t(f_{C(t)}^*))}_{\text{Estimation Regret}} \quad (37)$$

- **Identification Regret:** This term captures the loss incurred from selecting the wrong forecaster (i.e., $f_{\text{sel}}(t) \neq f_{\text{CEP}}(t)$). This occurs if the gene of an instance from concept C_k is closer to the gene of another forecaster f_j . The core strength of CEP lies in minimizing this regret. As long as the statistical genes \mathbf{z}_k of different concepts are well-separated in the feature space, the probability of misidentification is low. This regret is bounded by the number of misidentification events, which is minimal in scenarios with distinct concept shifts.
- **Estimation Regret:** This term reflects the cumulative loss because our online-trained forecasters are not the true optimal ones. CEP’s key innovation is converting a single non-stationary learning problem into a set of parallel, stationary subproblems. Each forecaster f_k in the pool is updated only with data from its corresponding concept C_k . For standard online learning algorithms (like online gradient descent) on a stationary distribution, the regret is known to be sublinear in the number of samples received, e.g., $O(\sqrt{T_k})$ Zinkevich (2003); Hazan et al. (2016) where T_k is the total number of instances seen for concept C_k . The total estimation regret is the sum of these sublinear regrets across all active forecasters.

By design, CEP excels at minimizing the Identification Regret through its statistically-grounded assignment mechanism. It effectively bounds the Estimation Regret by ensuring each specialized forecaster learns on a stable data distribution. Consequently, the total regret of CEP is expected to grow sublinearly with time, demonstrating its convergence towards the optimal dynamic strategy. This provides a strong theoretical justification for its superior performance over single-model approaches that suffer from catastrophic forgetting, which often leads to linear regret in concept drift settings.

C Experiment Details

C.1 Dataset

During the experiments, we used a diverse range of datasets to comprehensively assess the time series forecasting model. **ETT**, which covers two years, monitors the oil temperature and six power load characteristics. **ETT**h2

logs data hourly, while ETTm1 records at 15-minute intervals, presenting multiple granularities for the analysis of electricity-related time series. **Electricity (ECL)** dataset, which monitors the electricity consumption of 321 clients from 2012 to 2014, facilitates the exploration of intricate consumption patterns. **Weather (WTH)** monitored 11 climatic aspects at around 1,600 spots throughout the United States every hour from 2010 to 2013. **Traffic**, sourced from the California Department of Transportation, supplies hourly freeway occupancy rates in the San Francisco Bay Area, which is beneficial for traffic flow forecasting. **Exchange**, spanning from 1990 to 2016 and containing the daily exchange rates of eight countries, is instrumental in predicting the fluctuations in the foreign exchange market [Wu et al. \(2021\)](#). All the datasets were used with a single channel with the recurring concept shift in [Table 5](#). In the experiment, the ratio of the data set in the warm-up stage and online stage is 25 : 75.

Table 5 Dataset statistics.

Data	ECL	ETTh1	ETTh2	ETTm1	ETTm2	Exchange	Traffic	WTH
Feature	MT_104	LULL	LUFL	LULL	MUFL	OT	16	DewPointFahrenheit
Timestep	26,304	14,400	14,400	14,400	14,400	7,588	17,544	35,064

C.2 Experimental Setting

The experiments were conducted on a computer equipped with an AMD Ryzen 9 7950X CPU, which boasts 16 cores and a clock speed of 5.1 GHz. This computer is furnished with 64 GB of memory, and all experiments were executed using PyTorch. The default hyperparameters of CEP are presented in [Table 6](#). The details regarding the hyperparameter sensitivity are provided in [Section C.8](#).

Table 6 Hyparameters of CEP in the experiments.

Hyperparameter	τ_μ	τ_{gene}	τ_l	τ_{safe}	τ_e
Value	3.0	0.8	0.2	15	1.5

C.2.1 Gradual Concept Drift

To assess model adaptability to gradual distribution shifts, we set the forecast horizon to $\mathbf{H} = 1$. Our results show that no single online method consistently excels. A base model achieved state-of-the-art (SOTA) results on four datasets, matching the performance of an experience replay-based method [Buzzega et al. \(2020\)](#). Other methods like FSNet [Pham et al. \(2023\)](#) and OneNet [Zhang et al. \(2023\)](#) proved less effective in this gradual shift scenario. Given that all models produced low and acceptable errors, we conclude that sophisticated techniques for handling gradual concept drift are unnecessary for short-term forecasting.

When the forecasting horizon $\mathbf{H} = 1$, each input instance updates only one time step. This leads to only minor alterations in the overall input data, resulting in a gradual concept shift. We conducted experiments with $\mathbf{H} = 1$ using previous online methods and base forecasters with different common backbones. Additionally, we applied the CEP to the base forecasters. The specific experimental results are presented in [Table 7](#). From the experimental results, it is evident that the online time series forecasting methods did not demonstrate an absolute advantage over the base forecasters. Both achieved state-of-the-art (SOTA) performance in four datasets.

C.3 Full Experiment Result of Base Forecasters

We conducted experiments with forecasting horizons set to $\mathbf{H} \in \{30, 60\}$. In each instance, at least half of the total input length is updated, preventing a gradual shift in the distribution. Consequently, the phenomenon of concept recurrence becomes more pronounced. The detailed experimental results are presented in [Table 8](#). These results demonstrate that CEP substantially enhances the prediction performance of the base forecaster. To more intuitively illustrate the forecasting effect of CEP, the forecasting results of CEP and the base forecasters are depicted in [Figure 7](#).

Table 7 Full MSE errors of gradual concept shift experiments. Enhanced and reduced outcomes are marked with and respectively. The **best** and second-best performances are highlighted.

Data	ECL		ETTh1		ETTh2		ETTm1		ETTm2		Exchange		Traffic		WTH	
	MSE	Std														
ER	0.124	0.004	0.084	0.001	0.693	0.006	0.089	0.000	0.050	0.000	0.189	0.025	0.606	0.361	0.091	0.015
DER++	0.107	0.004	0.081	0.001	0.663	0.006	0.086	0.000	0.048	0.000	0.168	0.020	0.507	0.321	0.072	0.012
FSNet	0.208	0.026	0.091	0.001	0.767	0.010	0.123	0.009	0.062	0.001	1.175	0.425	0.618	0.065	0.096	0.004
OneNet	0.109	0.004	0.084	0.001	0.737	0.021	0.115	0.005	0.058	0.002	0.248	0.321	0.303	0.015	0.065	0.002
TCN	0.070	0.003	0.079	0.001	0.701	0.006	0.094	0.001	0.053	0.001	0.033	0.001	0.190	0.011	0.045	0.000
+CEP \times	0.070	0.003	0.079	0.001	0.701	0.006	0.094	0.001	0.053	0.001	0.033	0.001	0.190	0.011	0.045	0.000
TimesNet	0.096	0.009	0.110	0.010	0.888	0.045	0.185	0.012	0.093	0.010	0.077	0.009	0.329	0.028	0.077	0.005
+CEP \times	0.096	0.009	0.110	0.010	0.901	0.071	0.192	0.014	0.093	0.010	0.077	0.008	0.329	0.028	0.077	0.005
DLinear	0.160	0.000	0.109	0.000	1.026	0.001	0.218	0.000	0.069	0.000	0.077	0.000	0.251	0.000	0.061	0.000
+CEP \times	0.160	0.000	0.109	0.000	1.026	0.001	0.223	0.001	0.069	0.000	0.077	0.000	0.251	0.000	0.061	0.000
PatchTST	0.105	0.013	0.096	0.007	0.966	0.108	0.142	0.019	0.068	0.004	0.066	0.009	0.284	0.039	0.072	0.017
+CEP \times	0.105	0.013	0.095	0.006	0.993	0.102	0.151	0.026	0.071	0.008	0.067	0.007	0.284	0.039	0.067	0.015
iTransformer	0.126	0.033	0.117	0.009	0.956	0.042	0.239	0.047	0.089	0.007	0.083	0.010	0.308	0.015	0.108	0.015
+CEP \times	0.123	0.023	0.116	0.009	0.950	0.050	0.221	0.052	0.089	0.007	0.095	0.029	0.305	0.012	0.108	0.015
TimeMixer	0.066	0.005	0.091	0.005	0.701	0.018	0.113	0.007	0.060	0.002	0.040	0.004	0.263	0.016	0.050	0.003
+CEP \times	0.066	0.005	0.091	0.005	0.702	0.016	0.114	0.007	0.060	0.002	0.039	0.003	0.263	0.016	0.051	0.002

Table 8 Full MSE errors of different forecasters when using CEP are presented. Enhanced and reduced outcomes are marked with and respectively.

Data	MSE															
	ECL		ETTh1		ETTh2		ETTm1		ETTm2		Exchange		Traffic		WTH	
	30	60	30	60	30	60	30	60	30	60	30	60	30	60	30	60
TimeMixer	0.266	0.314	0.295	0.376	2.112	3.149	0.577	0.933	0.219	0.255	0.245	0.466	0.433	0.524	0.313	0.399
+CEP \times	0.244	0.297	0.274	0.371	2.000	3.016	0.579	0.895	0.216	0.254	0.233	0.450	0.433	0.524	0.313	0.396
	-8.34%	-5.17%	-7.13%	-1.38%	-5.29%	-4.21%	0.38%	-4.10%	-1.19%	-0.39%	-5.13%	-3.43%	0.00%	0.00%	0.00%	-0.55%
iTransformer	0.254	0.296	0.280	0.371	1.974	3.159	0.606	0.915	0.212	0.267	0.274	0.495	0.437	0.534	0.311	0.395
+CEP \times	0.229	0.282	0.275	0.372	1.968	3.116	0.594	0.886	0.210	0.265	0.249	0.484	0.437	0.534	0.311	0.394
	-9.62%	-4.72%	-2.00%	0.11%	-0.27%	-1.34%	-1.98%	-3.08%	-1.22%	-0.45%	-9.33%	-2.18%	0.00%	0.00%	0.00%	-0.40%
PatchTST	0.279	0.340	0.284	0.380	2.028	3.160	0.607	0.911	0.209	0.265	0.263	0.479	0.582	0.589	0.310	0.398
+CEP \times	0.265	0.328	0.276	0.377	1.922	2.995	0.567	0.875	0.208	0.264	0.234	0.467	0.582	0.589	0.310	0.397
	-5.01%	-3.70%	-2.81%	-0.95%	-5.26%	-5.22%	-6.55%	-3.97%	-0.67%	-0.45%	-11.25%	-2.51%	0.00%	0.00%	0.00%	-0.40%
DLinear	0.275	0.340	0.289	0.385	2.070	3.366	0.656	1.042	0.200	0.271	0.292	0.523	0.614	0.641	0.295	0.388
+CEP \times	0.264	0.335	0.259	0.356	2.052	3.209	0.586	0.917	0.196	0.259	0.261	0.494	0.614	0.641	0.295	0.386
	-4.07%	-1.41%	-10.38%	-7.43%	-0.88%	-4.65%	-10.69%	-12.05%	-2.00%	-4.36%	-10.69%	-5.62%	0.00%	0.00%	0.00%	-0.62%
SegRNN	0.242	0.314	0.250	0.356	1.864	3.391	0.554	0.883	0.201	0.263	0.193	0.397	0.693	0.930	0.298	0.384
+CEP \times	0.239	0.312	0.248	0.353	1.840	3.328	0.551	0.881	0.197	0.259	0.192	0.395	0.693	0.930	0.298	0.385
	-1.08%	-0.57%	-0.80%	-0.73%	-1.26%	-1.88%	-0.58%	-0.16%	-1.89%	-1.82%	-0.52%	-0.50%	0.00%	0.00%	0.00%	0.36%
TimesNet	0.281	0.330	0.304	0.398	2.141	3.212	0.692	0.981	0.237	0.279	0.297	0.546	0.492	0.597	0.323	0.406
+CEP \times	0.259	0.319	0.291	0.390	2.054	3.065	0.639	0.947	0.234	0.277	0.259	0.530	0.492	0.597	0.323	0.404
	-7.77%	-3.27%	-4.08%	-2.11%	-4.04%	-4.59%	-7.60%	-3.53%	-1.35%	-0.79%	-13.05%	-3.07%	0.00%	0.00%	0.00%	-0.49%
TCN	0.295	0.393	0.371	0.555	2.493	3.838	0.761	1.201	0.221	0.320	0.389	0.694	0.668	0.714	0.314	0.439
+CEP \times	0.261	0.358	0.392	0.526	2.164	3.443	0.638	0.964	0.219	0.309	0.272	0.553	0.668	0.714	0.314	0.450
	-11.71%	-9.00%	5.88%	-5.19%	-13.20%	-10.29%	-16.21%	-19.79%	-0.81%	-3.62%	-30.25%	-20.33%	0.00%	0.00%	0.00%	2.46%
Data	Std															
	ECL		ETTh1		ETTh2		ETTm1		ETTm2		Exchange		Traffic		WTH	
	30	60	30	60	30	60	30	60	30	60	30	60	30	60	30	60
TimeMixer	0.006	0.003	0.016	0.006	0.060	0.032	0.027	0.019	0.020	0.018	0.010	0.013	0.018	0.033	0.002	0.003
+CEP \times	0.007	0.003	0.005	0.005	0.013	0.006	0.025	0.010	0.022	0.018	0.011	0.014	0.018	0.033	0.002	0.003
iTransformer	0.004	0.003	0.002	0.004	0.014	0.027	0.010	0.012	0.002	0.003	0.010	0.008	0.012	0.009	0.002	0.001
+CEP \times	0.004	0.001	0.002	0.004	0.009	0.036	0.012	0.020	0.002	0.003	0.003	0.009	0.012	0.009	0.002	0.002
PatchTST	0.004	0.002	0.001	0.005	0.018	0.035	0.014	0.012	0.005	0.007	0.002	0.011	0.006	0.004	0.001	0.001
+CEP \times	0.002	0.004	0.004	0.004	0.015	0.019	0.007	0.008	0.005	0.007	0.006	0.012	0.006	0.004	0.001	0.001
DLinear	0.000	0.001	0.001	0.002	0.002	0.002	0.002	0.001	0.001	0.006	0.012	0.013	0.001	0.000	0.000	0.000
+CEP \times	0.001	0.000	0.000	0.001	0.003	0.003	0.002	0.001	0.001	0.006	0.010	0.013	0.001	0.000	0.000	0.000
SegRNN	0.003	0.003	0.001	0.002	0.006	0.011	0.001	0.004	0.003	0.002	0.001	0.000	0.013	0.026	0.002	0.001
+CEP \times	0.003	0.003	0.001	0.002	0.004	0.006	0.002	0.003	0.003	0.002	0.001	0.000	0.013	0.026	0.002	0.002
TimesNet	0.01															

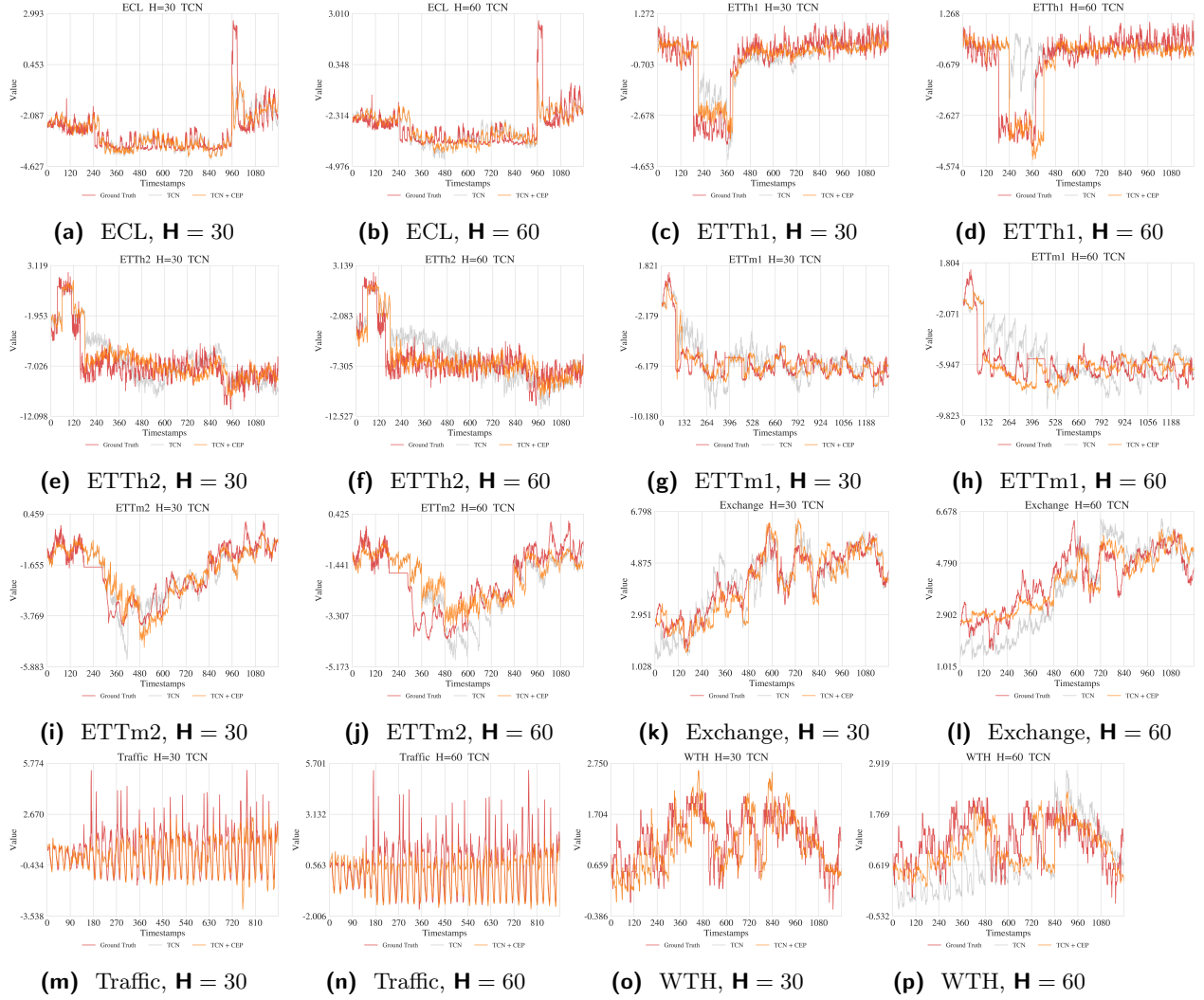


Figure 7 Visualization of results by base forecasters *vs.* forecasters with CEP across all datasets

C.4 Full Experiment Result of Online Methods

All online methods incorporate the same TCN component. We compare the performance of online methods, the base TCN, and the TCN utilizing CEP. The full experimental results are presented in Table 9. An intriguing phenomenon is that, in comparison to the base TCN, online methods nearly fail in most scenarios. A plausible explanation is that, owing to delayed feedback, the information acquired by online methods is delayed and fails to adapt promptly to concept changes. The CEP significantly enhances the performance of TCN, effectively reducing prediction errors across a wide range of datasets.

C.5 Ablation Study

In the ablation experiment, we tested the mechanisms in the CEP. These mechanisms include evolution, using only local Genes, using only Global Genes, elimination, inspiration, and gradient abandonment. We tested all the forecasters and took the average of the results. The specific experimental results are in Table 10. The most basic evolution mechanism in the CEP played a major role when compared to the performance without CEP. Other mechanisms show limited effectiveness for two reasons. First, the performance of different forecasters can vary under the influence of CEP, and second, the use of uniform default parameters limits the effectiveness of the datasets with different characteristics.

Table 9 Full MSE error of previous online forecasting methods. The **best** and second-best performances are highlighted.

MSE																
Data	ECL		ETTh1		ETTh2		ETTh1		ETTh2		Exchange		Traffic		WTH	
	30	60	30	60	30	60	30	60	30	60	30	60	30	60	30	60
TCN 	<u>0.295</u>	<u>0.393</u>	0.371	0.555	2.493	3.838	<u>0.761</u>	<u>1.201</u>	<u>0.221</u>	<u>0.320</u>	<u>0.389</u>	<u>0.694</u>	0.668	<u>0.714</u>	0.314	0.439
ER	0.563	0.685	0.358	0.551	2.624	4.035	0.901	1.862	0.246	0.399	2.268	3.550	1.359	0.862	0.524	0.592
DER++	0.538	0.621	0.332	<u>0.481</u>	<u>2.339</u>	<u>3.806</u>	0.804	1.622	0.235	0.373	1.568	3.462	1.325	0.827	0.486	0.573
FSNet	0.863	0.822	0.392	0.547	3.118	5.025	1.111	2.013	0.275	0.419	3.093	3.879	1.618	1.314	0.641	0.846
OneNet	0.385	0.466	<u>0.344</u>	0.475	2.540	4.265	0.949	1.237	0.237	0.332	0.899	1.361	<u>0.705</u>	0.640	<u>0.360</u>	0.469
CEP 	0.261	0.358	0.392	0.526	2.164	3.443	0.638	0.964	0.219	0.309	0.272	0.553	0.668	<u>0.714</u>	0.314	<u>0.450</u>

Std																
Data	ECL		ETTh1		ETTh2		ETTh1		ETTh2		Exchange		Traffic		WTH	
	30	60	30	60	30	60	30	60	30	60	30	60	30	60	30	60
TCN	0.010	0.005	0.015	0.044	0.021	0.083	0.006	0.031	0.019	0.011	0.009	0.018	0.070	0.006	0.002	0.004
ER	0.006	0.050	0.002	0.026	0.116	0.040	0.016	0.058	0.006	0.005	0.243	0.684	0.283	0.048	0.014	0.012
DER++	0.015	0.055	0.007	0.034	0.126	0.070	0.013	0.068	0.007	0.007	0.847	0.364	0.278	0.048	0.014	0.012
FSNet	0.108	0.044	0.014	0.027	0.042	0.088	0.008	0.060	0.019	0.012	0.335	0.508	0.093	0.147	0.055	0.042
OneNet	0.011	0.036	0.013	0.016	0.068	0.254	0.034	0.099	0.013	0.027	0.179	0.151	0.029	0.018	0.011	0.014
CEP	0.009	0.007	0.013	0.058	0.053	0.107	0.006	0.052	0.021	0.012	0.019	0.016	0.070	0.006	0.002	0.003

Table 10 Full ablation study results. All results are the averaged MSE of different backbone forecasters. The **best** and second-best performances are highlighted.

Evolution	Inspiration	Gradient Abandonment	Elimination	Local Gene	Global Gene	ECL		ETTh1		ETTh2		ETTh1		ETTh2		Exchange		Traffic		WTH		AVG	Rank	
						30	60	30	60	30	60	30	60	30	60	30	60	30	60	30	60			30
						0.295	0.398	0.359	0.512	2.480	3.732	0.753	1.228	0.208	0.313	0.361	0.687	0.696	0.724	0.313	0.437	0.844	25	
✓	✗	✗	✓	✗	✓	0.275	0.377	0.332	0.477	2.339	3.845	<u>0.627</u>	0.929	0.219	0.309	0.361	0.687	0.696	0.724	0.313	0.437	0.809	24	
✓	✗	✗	✗	✓	✓	0.294	0.392	0.332	<u>0.446</u>	2.339	3.814	<u>0.627</u>	0.929	0.219	0.309	0.361	0.687	0.696	0.724	0.313	0.437	0.807	23	
✓	✗	✗	✓	✓	✗	0.271	0.373	0.330	0.443	2.368	3.958	<u>0.627</u>	0.988	0.207	0.309	0.288	0.579	0.696	0.724	0.312	0.415	0.806	22	
✓	✗	✓	✓	✓	✓	0.275	0.379	0.348	0.480	2.353	3.688	<u>0.650</u>	<u>0.935</u>	0.210	<u>0.305</u>	0.361	0.687	0.696	0.724	0.313	0.437	0.803	21	
✓	✗	✗	✗	✓	✓	0.281	0.383	0.330	0.443	2.323	3.886	<u>0.627</u>	<u>0.988</u>	0.204	0.309	0.291	0.567	0.696	0.724	0.307	0.410	0.798	20	
✓	✗	✓	✗	✓	✓	0.296	0.408	0.348	0.462	2.353	3.565	0.650	<u>0.935</u>	0.217	<u>0.305</u>	0.361	0.687	0.696	0.724	0.313	0.437	0.797	19	
✓	✗	✗	✗	✓	✓	0.289	0.378	0.330	0.443	2.393	3.815	<u>0.627</u>	0.929	0.213	0.309	0.298	<u>0.525</u>	0.696	0.724	0.313	0.434	0.795	18	
✓	✗	✗	✓	✓	✓	0.274	0.377	0.330	0.443	2.366	3.832	<u>0.627</u>	0.929	0.207	0.309	0.292	<u>0.525</u>	0.696	0.724	0.313	0.434	0.792	17	
✓	✓	✓	✓	✓	✗	0.270	0.363	0.397	0.505	2.204	3.604	0.628	0.973	0.212	0.302	0.361	0.687	0.696	0.724	0.313	0.437	0.792	16	
✓	✓	✓	✓	✓	✗	0.268	0.370	0.379	0.490	2.314	3.641	0.596	1.059	0.208	0.307	0.267	0.564	0.696	0.724	0.310	0.422	0.788	15	
✓	✓	✓	✓	✓	✗	0.271	0.358	0.373	0.493	2.160	3.651	0.596	0.936	0.215	0.307	0.361	0.687	0.696	0.724	0.313	0.437	0.786	14	
✓	✓	✗	✓	✓	✓	0.281	0.392	<u>0.331</u>	0.447	2.311	3.665	0.650	1.026	<u>0.205</u>	<u>0.305</u>	0.291	0.534	0.696	0.724	0.307	<u>0.411</u>	0.786	13	
✓	✓	✗	✓	✓	✓	0.297	0.394	0.373	0.489	2.160	3.550	0.596	0.936	0.208	0.307	0.361	0.687	0.696	0.724	0.313	0.437	0.783	12	
✓	✓	✓	✓	✓	✓	0.269	0.378	<u>0.331</u>	0.447	2.353	3.577	0.650	1.026	0.207	<u>0.305</u>	0.287	0.545	0.696	0.724	0.313	0.416	0.783	11	
✓	✓	✓	✓	✓	✗	0.298	0.412	0.397	0.506	2.204	3.368	0.628	0.973	<u>0.205</u>	0.302	0.361	0.687	0.696	0.724	0.313	0.437	0.782	10	
✓	✓	✗	✓	✓	✓	0.286	0.387	<u>0.331</u>	0.447	2.334	3.651	0.650	<u>0.935</u>	0.207	<u>0.305</u>	0.288	0.518	0.696	0.724	0.313	0.438	0.782	9	
✓	✓	✓	✓	✓	✓	0.264	0.378	0.380	0.495	2.313	3.431	0.628	1.102	0.209	0.302	0.269	0.533	0.696	0.724	0.310	0.424	0.779	8	
✓	✓	✓	✓	✓	✗	0.278	0.371	0.379	0.490	2.255	3.526	0.596	1.059	<u>0.205</u>	0.307	0.272	0.561	0.696	0.724	0.302	0.414	0.777	7	
✓	✓	✓	✓	✓	✗	0.277	0.383	0.380	0.495	2.255	3.425	0.628	1.102	0.206	0.302	0.274	0.526	0.696	0.724	<u>0.303</u>	0.414	0.774	6	
✓	✓	✗	✓	✓	✓	0.271	0.380	<u>0.331</u>	0.447	2.318	3.570	0.650	<u>0.935</u>	0.207	<u>0.305</u>	0.283	0.518	0.696	0.724	0.313	0.438	0.774	5	
✓	✓	✓	✓	✓	✓	0.273	<u>0.359</u>	0.379	0.490	<u>2.165</u>	3.592	0.596	0.936	0.208	0.307	<u>0.266</u>	0.542	0.696	0.724	0.313	0.440	0.768	4	
✓	✓	✓	✓	✓	✓	0.286	0.377	0.379	0.490	2.191	3.531	0.596	0.936	0.208	0.307	0.269	0.542	0.696	0.724	0.313	0.440	0.768	3	
✓	✓	✓	✓	✓	✓	0.281	0.389	0.380	0.495	2.187	<u>3.406</u>	0.628	0.973	0.206	0.302	<u>0.266</u>	0.546	0.696	0.724	0.313	0.445	<u>0.765</u>	<u>2</u> 	
						CEP 	<u>0.265</u>	0.363	0.380	0.495	2.174	3.424	0.628	0.973	0.209	0.302	0.262	0.546	0.696	0.724	0.313	0.445	0.762	1 

C.6 Full Experiment Result of Forecaster Assignment Mechanisms

To justify the design choice of the deterministic Nearest Retrieval mechanism in CEP, we compare it against standard MoE gating strategies Shazeer et al. (2017). Specifically, we implemented two variants of the gating network using the same backbone forecasters: (1) **Softmax Gating**: A trainable multi-layer perceptron that outputs a probability distribution over experts, using the weighted sum of their outputs; (2) **Noisy Top-K Gating**: A standard sparse MoE approach that adds Gaussian noise to the gating logits and activates only the top-k experts. In our experimental setup, the number of experts was set to 3 with $K = 2$.

The experimental results, comparing MSE and model size, are presented in Table 11 and Table 12. The results indicate that CEP consistently outperforms differentiable gating mechanisms in the context of recurring concept drift. We attribute this performance gap to the phenomenon of **Gradient Pollution** in online learning. In a Softmax Gating scenario, backpropagation updates all experts with non-zero weights for every incoming instance. Consequently, an expert specialized in a historical concept (e.g., a specific seasonal pattern) is continuously modified by gradients from the current, unrelated concept, leading to the catastrophic forgetting of its specialized knowledge. However, in datasets where CEP intervenes less frequently, such as Traffic and Weather, Softmax gating proves effective. Notably, differentiable gating is not inherently incompatible with CEP; future work could explore a combined approach that integrates CEP’s pool management with Softmax gating. Even with Noisy Top-K gating, the stochastic nature of the gate can inadvertently activate and overwrite the wrong expert during transition periods.

In contrast, CEP employs a gene-based assignment strategy. By strictly freezing the parameters of inactive forecasters based on statistical distance in the gene space, CEP ensures **Parameter Isolation**. This allows specific experts to remain dormant and pristine until their specific concept recurs, effectively solving the interference problem inherent in soft-gating mechanisms while maintaining a comparable or smaller memory footprint.

Table 11 Full MSE error of comparison of the assignment mechanisms. The **best** performances are highlighted.

Data		ECL		ETTh1		ETTh2		ETTm1		ETTm2		Exchange		Traffic		WTH		Count
		30	60	30	60	30	60	30	60	30	60	30	60	30	60	30	60	
TCN	Gene \boxtimes	0.265	0.363	0.380	0.495	2.174	3.424	0.628	0.973	0.209	0.302	0.262	0.546	0.696	0.724	0.313	0.445	10
	Softmax	0.276	0.424	0.404	0.550	2.684	4.278	0.919	1.327	0.207	0.325	0.408	0.700	0.612	0.636	0.307	0.417	3
	Noisy Top-K	0.285	0.393	0.397	0.460	2.541	3.745	0.804	1.228	0.206	0.337	0.329	0.654	0.583	0.681	0.316	0.417	4
TimesNet	Gene \boxtimes	0.259	0.311	0.279	0.387	2.009	3.140	0.631	0.938	0.236	0.269	0.256	0.460	0.524	0.619	0.325	0.409	8
	Softmax	0.279	0.300	0.288	0.396	2.261	3.066	0.760	0.952	0.238	0.284	0.353	0.585	0.543	0.576	0.314	0.397	4
	Noisy Top-K	0.276	0.322	0.295	0.371	2.016	3.224	0.641	0.924	0.223	0.285	0.308	0.520	0.531	0.542	0.329	0.412	4
SegRNN	Gene \boxtimes	0.238	0.310	0.248	0.351	1.843	3.321	0.550	0.880	0.196	0.260	0.192	0.395	0.670	0.899	0.297	0.387	7
	Softmax	0.240	0.303	0.254	0.351	1.927	3.401	0.523	0.785	0.186	0.227	0.194	0.396	0.630	0.804	0.287	0.376	10
	Noisy Top-K	0.243	0.311	0.255	0.372	1.894	3.454	0.528	0.813	0.194	0.253	0.194	0.394	0.653	0.813	0.292	0.382	0
DLinear	Gene \boxtimes	0.264	0.334	0.259	0.356	2.051	3.208	0.586	0.916	0.198	0.269	0.272	0.489	0.614	0.641	0.295	0.386	11
	Softmax	0.281	0.344	0.292	0.415	2.072	3.396	0.740	0.961	0.203	0.261	0.301	0.589	0.522	0.543	0.291	0.374	4
	Noisy Top-K	0.278	0.362	0.285	0.380	2.315	3.427	0.707	0.960	0.203	0.276	0.295	0.542	0.519	0.554	0.295	0.379	1
PatchTST	Gene \boxtimes	0.264	0.324	0.270	0.379	1.915	3.017	0.558	0.881	0.216	0.274	0.234	0.457	0.587	0.588	0.311	0.396	9
	Softmax	0.288	0.345	0.311	0.380	2.074	3.113	0.627	0.884	0.197	0.263	0.256	0.528	0.569	0.564	0.303	0.389	6
	Noisy Top-K	0.289	0.322	0.291	0.386	2.096	3.052	0.588	0.899	0.209	0.265	0.269	0.472	0.583	0.612	0.307	0.399	1
iTransformer	Gene \boxtimes	0.231	0.283	0.274	0.379	1.962	3.083	0.582	0.881	0.206	0.265	0.250	0.474	0.449	0.524	0.314	0.395	7
	Softmax	0.252	0.303	0.275	0.375	1.941	3.057	0.608	0.883	0.202	0.272	0.280	0.492	0.428	0.469	0.301	0.386	3
	Noisy Top-K	0.245	0.304	0.272	0.373	1.980	3.236	0.595	0.844	0.199	0.279	0.264	0.520	0.421	0.470	0.306	0.394	6
TimeMixer	Gene \boxtimes	0.242	0.299	0.276	0.371	2.007	3.021	0.620	0.889	0.223	0.241	0.251	0.431	0.456	0.495	0.315	0.393	6
	Softmax	0.270	0.351	0.317	0.413	2.168	3.054	0.613	0.883	0.226	0.240	0.240	0.518	0.410	0.490	0.309	0.391	7
	Noisy Top-K	0.269	0.309	0.283	0.406	1.984	3.095	0.587	0.907	0.199	0.245	0.256	0.488	0.439	0.571	0.318	0.401	3

Table 12 Full weight sizes (MB) of assignment mechanisms. The **smallest** sizes are highlighted.

Data		ECL		ETTh1		ETTh2		ETTm1		ETTm2		Exchange		Traffic		WTH		Count
		30	60	30	60	30	60	30	60	30	60	30	60	30	60	30	60	
TCN	Gene ⌘	9.89	9.91	9.87	9.89	19.72	19.78	19.71	19.77	9.87	9.89	29.56	19.78	9.87	9.89	9.89	19.79	15
	Softmax	29.50	29.61	29.50	29.61	29.50	29.61	29.50	29.61	29.50	29.61	29.50	29.61	29.50	29.61	29.50	29.61	1
	Noisy Top-K	29.50	29.61	29.50	29.61	29.50	29.61	29.50	29.61	29.50	29.61	29.50	29.61	29.50	29.61	29.50	29.61	1
TimesNet	Gene ⌘	2.64	2.63	2.62	2.62	5.22	5.22	5.21	5.21	2.62	2.62	7.80	5.21	2.62	2.62	2.65	5.23	15
	Softmax	7.77	7.79	7.77	7.79	7.77	7.79	7.77	7.79	7.77	7.79	7.77	7.79	7.77	7.79	7.77	7.79	1
	Noisy Top-K	7.77	7.80	7.77	7.80	7.77	7.80	7.77	7.80	7.77	7.80	7.77	7.80	7.77	7.80	7.77	7.80	1
SegRNN	Gene ⌘	0.09	0.06	0.07	0.06	0.11	0.10	0.10	0.09	0.07	0.06	0.14	0.09	0.07	0.05	0.09	0.11	15
	Softmax	0.12	0.12	0.12	0.12	0.12	0.12	0.12	0.12	0.12	0.12	0.12	0.12	0.12	0.12	0.12	0.12	1
	Noisy Top-K	0.12	0.12	0.12	0.12	0.12	0.12	0.12	0.12	0.12	0.12	0.12	0.12	0.12	0.12	0.12	0.12	1
DLinear	Gene ⌘	0.07	0.06	0.05	0.05	0.07	0.09	0.07	0.08	0.05	0.05	0.08	0.08	0.05	0.05	0.08	0.10	15
	Softmax	0.06	0.10	0.06	0.10	0.06	0.10	0.06	0.10	0.06	0.10	0.06	0.10	0.06	0.10	0.06	0.10	1
	Noisy Top-K	0.06	0.10	0.06	0.10	0.06	0.10	0.06	0.10	0.06	0.10	0.06	0.10	0.06	0.10	0.06	0.10	1
PatchTST	Gene ⌘	0.80	0.81	0.79	0.80	1.55	1.59	1.54	1.58	0.79	0.80	2.29	1.58	0.79	0.80	0.81	1.60	15
	Softmax	2.27	2.35	2.27	2.35	2.27	2.35	2.27	2.35	2.27	2.35	2.27	2.35	2.27	2.35	2.27	2.35	1
	Noisy Top-K	2.27	2.35	2.27	2.35	2.27	2.35	2.27	2.35	2.27	2.35	2.27	2.35	2.27	2.35	2.27	2.35	1
iTransformer	Gene ⌘	0.17	0.16	0.16	0.15	0.29	0.29	0.28	0.28	0.16	0.15	0.41	0.28	0.16	0.15	0.18	0.30	15
	Softmax	0.38	0.39	0.38	0.39	0.38	0.39	0.38	0.39	0.38	0.39	0.38	0.39	0.38	0.39	0.38	0.39	1
	Noisy Top-K	0.38	0.39	0.38	0.39	0.38	0.39	0.38	0.39	0.38	0.39	0.38	0.39	0.38	0.39	0.38	0.39	1
TimeMixer	Gene ⌘	1.00	1.00	0.99	1.00	1.95	1.98	1.94	1.97	0.99	0.99	2.89	1.97	0.99	0.99	1.01	1.99	15
	Softmax	2.87	2.93	2.87	2.93	2.87	2.93	2.87	2.93	2.87	2.93	2.87	2.93	2.87	2.93	2.87	2.93	1
	Noisy Top-K	2.87	2.93	2.87	2.93	2.87	2.93	2.87	2.93	2.87	2.93	2.87	2.93	2.87	2.93	2.87	2.93	1

C.7 Full Experiment Result of Time Series Foundation Models

With the recent emergence of TSFMs, a natural question arises regarding the necessity of training specialized adapters from scratch. To investigate this, we compared CEP using lightweight backbones against latest versions of Foundation Models, including **Chronos 2** Ansari et al. (2024), **Moirai 2** Woo et al. (2024), and **TimesFM 2.5** Das et al. (2024). These foundation models were evaluated in a zero-Shot setting, adhering to their standard usage paradigm for unseen domains. The comparative forecasting errors are detailed in Table 13 and model sizes in Table 14. We observe two critical findings:

- The Generalist-Specialist Gap in Online Adaptation.** While TSFMs demonstrate impressive generalization capabilities, they struggle to adapt to the specific, high-frequency recurring drifts present in datasets like Traffic or Electricity without computationally expensive fine-tuning. CEP, by continuously evolving specialized experts dynamically, achieves significantly lower MSE such as reducing error by orders of magnitude in ETTh1 and Traffic. This validates that for specific, dynamic environments, a continuously adapting specialist often outperforms a static generalist.
- Resource and Privacy Constraints.** As shown in Table 14, the parameter count of TSFMs ranges from hundreds of millions to billions, requiring substantial computing resources for inference. In contrast, CEP maintains a compact pool of lightweight models (often <10MB total), making it suitable for edge deployment. Furthermore, CEP operates strictly within the local environment, satisfying privacy constraints where data cannot be uploaded to cloud-based foundation model services.

C.8 Hyperparameter Sensitivity

We conducted a detailed hyperparameter sensitivity analysis to evaluate the impact of CEP’s core mechanisms. Experiments were performed on the ETTm1 dataset with a forecasting horizon of $H = 30$. The results, presented in Figure 8, provide insights into the system’s behavior.

The analysis reveals that performance is most responsive to hyperparameters governing the lifecycle of

Table 13 Full MSE error of comparison of CEP and TSFM. The **best** performances are highlighted.

Data	ECL		ETTh1		ETTh2		ETTm1		ETTm2		Exchange		Traffic		WTH	
	30	60	30	60	30	60	30	60	30	60	30	60	30	60	30	60
TCN+CEP 	0.261	0.358	0.392	0.526	2.164	3.443	0.638	0.964	0.219	0.309	0.272	0.553	0.668	0.714	0.314	0.450
TimesNet+CEP 	0.259	0.319	0.291	0.390	2.054	3.065	0.639	0.947	0.234	0.277	0.259	0.530	0.492	0.597	0.323	0.404
SegRNN+CEP 	<u>0.239</u>	0.312	0.248	0.353	1.840	3.328	0.551	<u>0.881</u>	<u>0.197</u>	<u>0.259</u>	0.192	<u>0.395</u>	0.693	0.930	<u>0.298</u>	0.385
DLinear+CEP 	0.264	0.335	0.259	<u>0.356</u>	2.052	3.209	0.586	0.917	0.196	0.259	0.261	0.494	0.614	0.641	0.295	<u>0.386</u>
PatchTST+CEP 	0.265	0.328	0.276	0.377	1.922	2.995	<u>0.567</u>	0.875	0.208	0.264	0.234	0.467	0.582	0.589	0.310	0.397
iTransformer+CEP 	0.229	0.282	0.275	0.372	1.968	3.116	0.594	0.886	0.210	0.265	0.249	0.484	<u>0.437</u>	<u>0.534</u>	0.311	0.394
TimeMixer+CEP 	0.244	<u>0.297</u>	0.274	0.371	2.000	3.016	0.579	0.895	0.216	0.254	0.233	0.450	0.433	0.524	0.313	0.396
Chronos 2	0.315	0.394	0.250	0.399	1.909	3.287	0.665	1.087	0.311	0.525	0.208	0.389	0.559	0.668	0.367	0.553
Moirai 2.0	0.316	0.409	0.259	0.370	<u>1.769</u>	2.769	0.635	1.046	0.282	0.419	<u>0.204</u>	0.441	0.625	0.798	0.332	0.469
TimesFM 2.5	0.316	0.394	<u>0.249</u>	0.367	1.684	<u>2.790</u>	0.624	1.008	0.297	0.424	0.206	0.432	0.557	0.637	0.318	0.429

Table 14 Full weight sizes (MB) of CEP and TSFM.

Data	ECL		ETTh1		ETTh2		ETTm1		ETTm2		Exchange		Traffic		WTH		Rank
	30	60	30	60	30	60	30	60	30	60	30	60	30	60	30	60	
DLinear+CEP 	0.33	0.29	0.25	0.25	0.36	0.45	0.33	0.40	0.24	0.25	0.41	0.40	0.24	0.25	0.38	0.50	1
SegRNN+CEP 	0.43	0.32	0.35	0.28	0.56	0.50	0.52	0.46	0.34	0.28	0.70	0.46	0.34	0.27	0.47	0.56	2
iTransformer+CEP 	0.87	0.79	0.79	0.75	1.45	1.43	1.41	1.39	0.79	0.74	2.03	1.38	0.79	0.74	0.92	1.49	3
PatchTST+CEP 	4.02	4.04	3.94	4.01	7.74	7.95	7.71	7.90	3.94	4.00	11.47	7.89	3.94	4.00	4.07	8.00	4
TimeMixer+CEP 	5.02	5.01	4.94	4.98	9.73	9.89	9.70	9.84	4.93	4.97	14.45	9.83	4.93	4.97	5.06	9.94	5
TimesNet+CEP 	13.20	13.13	13.12	13.09	26.10	26.12	26.07	26.07	13.12	13.09	39.01	26.06	13.12	13.09	13.25	26.17	6
TCN+CEP 	49.46	49.54	49.34	49.46	98.60	98.92	98.57	98.87	49.34	49.45	147.79	98.88	49.33	49.45	49.47	98.97	8
Moirai 2.0	43.45	43.45	43.45	43.45	43.45	43.45	43.45	43.45	43.45	43.45	43.45	43.45	43.45	43.45	43.45	43.45	7
Chronos 2	455.79	455.79	455.79	455.79	455.79	455.79	455.79	455.79	455.79	455.79	455.79	455.79	455.79	455.79	455.79	455.79	9
TimesFM 2.5	882.32	882.32	882.32	882.32	882.32	882.32	882.32	882.32	882.32	882.32	882.32	882.32	882.32	882.32	882.32	882.32	10

forecasters. For the **Mean Threshold** (τ_μ), as shown in Figure 8(a), an optimal value exists around 2.0-3.0. A threshold that is too low causes excessive and unstable evolution for minor fluctuations, while a threshold that is too high prevents the model from adapting to genuine concept shifts. A similar balance is observed for the **Elimination Threshold** (τ_e) in Figure 8(c), where a moderate value is crucial to prune outdated forecasters without prematurely discarding useful ones. Parameters that control adaptation speed, such as the **Local Ratio** (τ_l) in Figure 8(f), also demonstrate a clear optimal range, highlighting the importance of balancing responsiveness to recent data.

Conversely, CEP exhibits considerable robustness to other parameters. For instance, the **Gene Ratio** (τ_g) in Figure 8(d) shows stable performance across a wide range of values, indicating that the framework is not overly dependent on the precise weighting between short-term and long-term statistical features. Overall, these findings confirm that while our default settings provide strong baseline performance, targeted tuning of the most sensitive parameters can further enhance results for specific data characteristics.

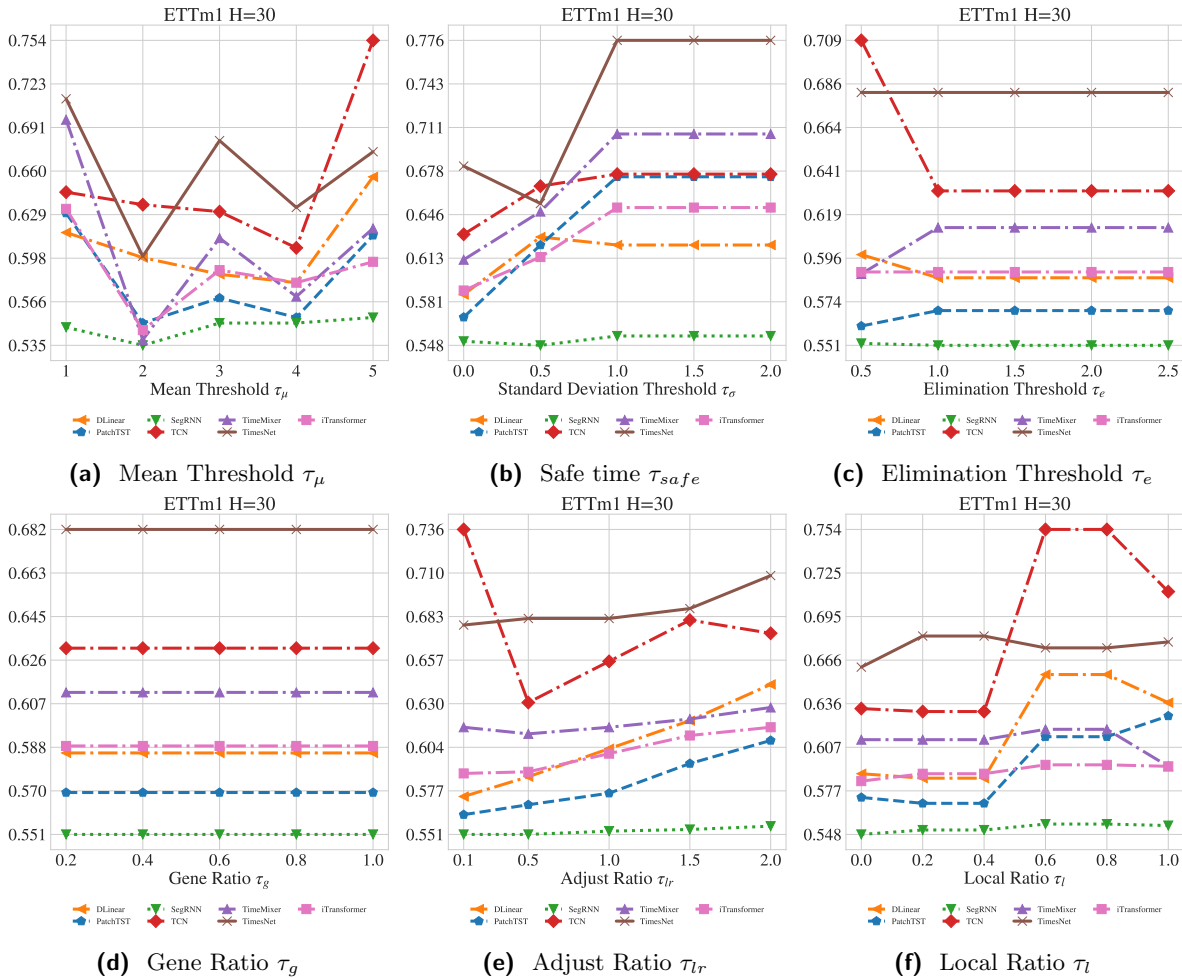


Figure 8 Results of Hyperparameter Sensitivity Analysis

C.9 Practical Usage Guide

While the default hyperparameters provide a robust starting point, performance can be further optimized by tuning them to the specific characteristics of a time series dataset. Based on our analysis, we provide the following practical guidance to help users configure CEP for their specific scenarios. Table 15 summarizes key hyperparameters, their effects, and our tuning recommendations.

Table 15 Practical guide for tuning CEP’s hyperparameters.

Hyperparameter	Description	Tuning Guidance
τ_μ	<i>Mean Threshold:</i> Controls sensitivity to shifts in the data’s mean value.	For noisy data or gradual drifts , use a higher value (e.g., 3.0-5.0) to prevent creating spurious forecasters. For abrupt, clear shifts , a lower value (e.g., 2.0-3.0) enables faster adaptation.
τ_e	<i>Elimination Threshold:</i> Determines how long an inactive forecaster is retained.	For concepts that recur after long intervals (e.g., annual seasonality), use a higher value to preserve this knowledge. If memory is a constraint or concepts are transient, a lower value keeps the pool lean.
τ_{safe}	<i>Safety Period:</i> The number of instances a new forecaster must see before it can evolve again.	For highly volatile or spiky data , a longer period ensures evolution is based on stable trends, not transient noise. For cleaner data, a shorter period allows for more rapid evolution if needed.
τ_{lr}	<i>LR Adjustment Ratio:</i> Sets the initial learning rate multiplier for a newly evolved forecaster.	A small value (e.g., 0.1-0.5) is generally recommended to enforce a sharp LR drop, promoting stable convergence on the new concept. Use larger values with caution as they risk unstable training.
τ_l	<i>Local Gene Ratio:</i> Controls how quickly the local gene adapts to new instances (EMA decay).	For rapidly changing environments , a higher value (e.g., 0.5-0.8) allows for faster tracking. For smoother trends , a lower value (e.g., 0.1-0.3) provides more stable local feature representation.

D Complexity Analysis

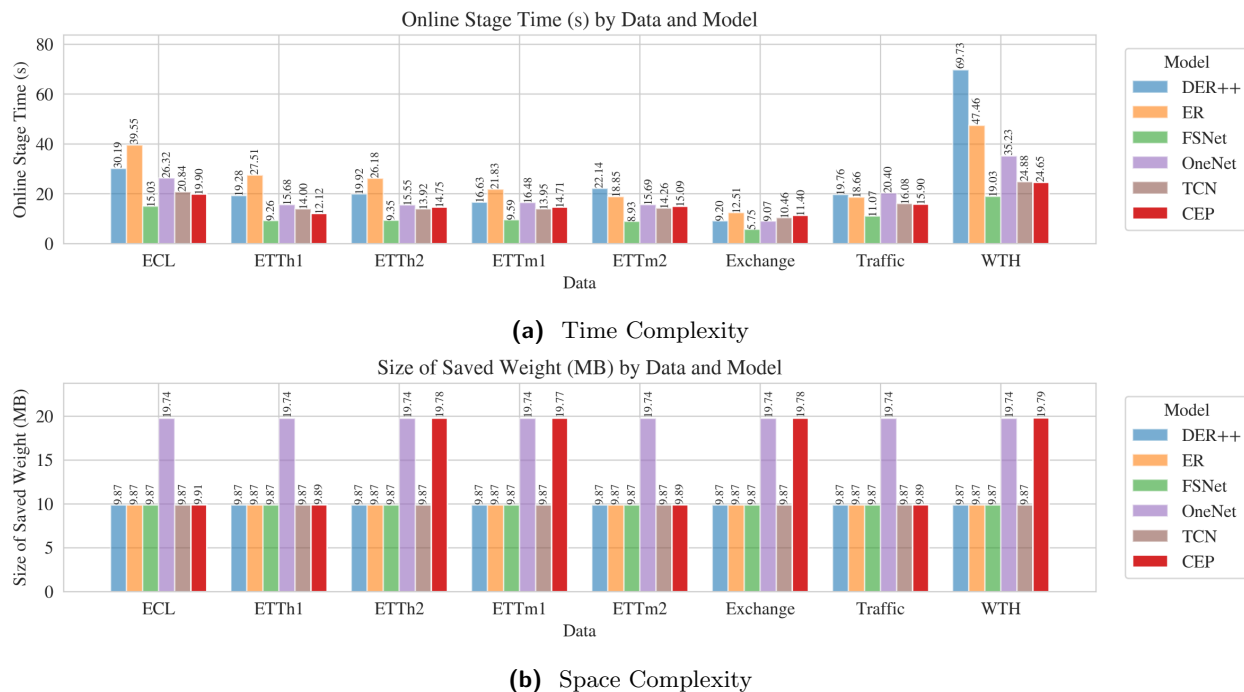


Figure 9 Computation Complexity of base TCN, online methods and CEP

Time Complexity. As shown in Figure 9a, the time complexity per prediction step is highly efficient. Since CEP activates only a single, specialized forecaster from the pool for any given instance, its inference time remains identical to that of the base forecaster model, denoted as $O(k)$. Here, k represents the computational operations required by the base model for a single input.

Space Complexity. The space complexity of CEP is actively managed to remain practical and efficient which is demonstrated in Figure 9b. While the theoretical worst-case space complexity could grow linearly with the total number of unique concepts encountered, $O(|\tilde{\mathcal{D}}| \cdot k)$, this scenario is effectively prevented by the integral *Forecaster Elimination* mechanism. This core component acts as a resource governor, dynamically pruning the pool by removing forecasters that correspond to transient, noisy, or outdated concepts that no longer recur.

Consequently, the actual memory footprint does not scale with the entire history of concepts but rather adapts to the number of *active and relevant* concepts in the current data regime. This design keeps the pool size bounded, ensuring the space complexity is manageable in practice. As empirically demonstrated in Figure 10, the number of active forecasters remains well-controlled throughout the online stage, confirming the effectiveness of this self-regulating mechanism.

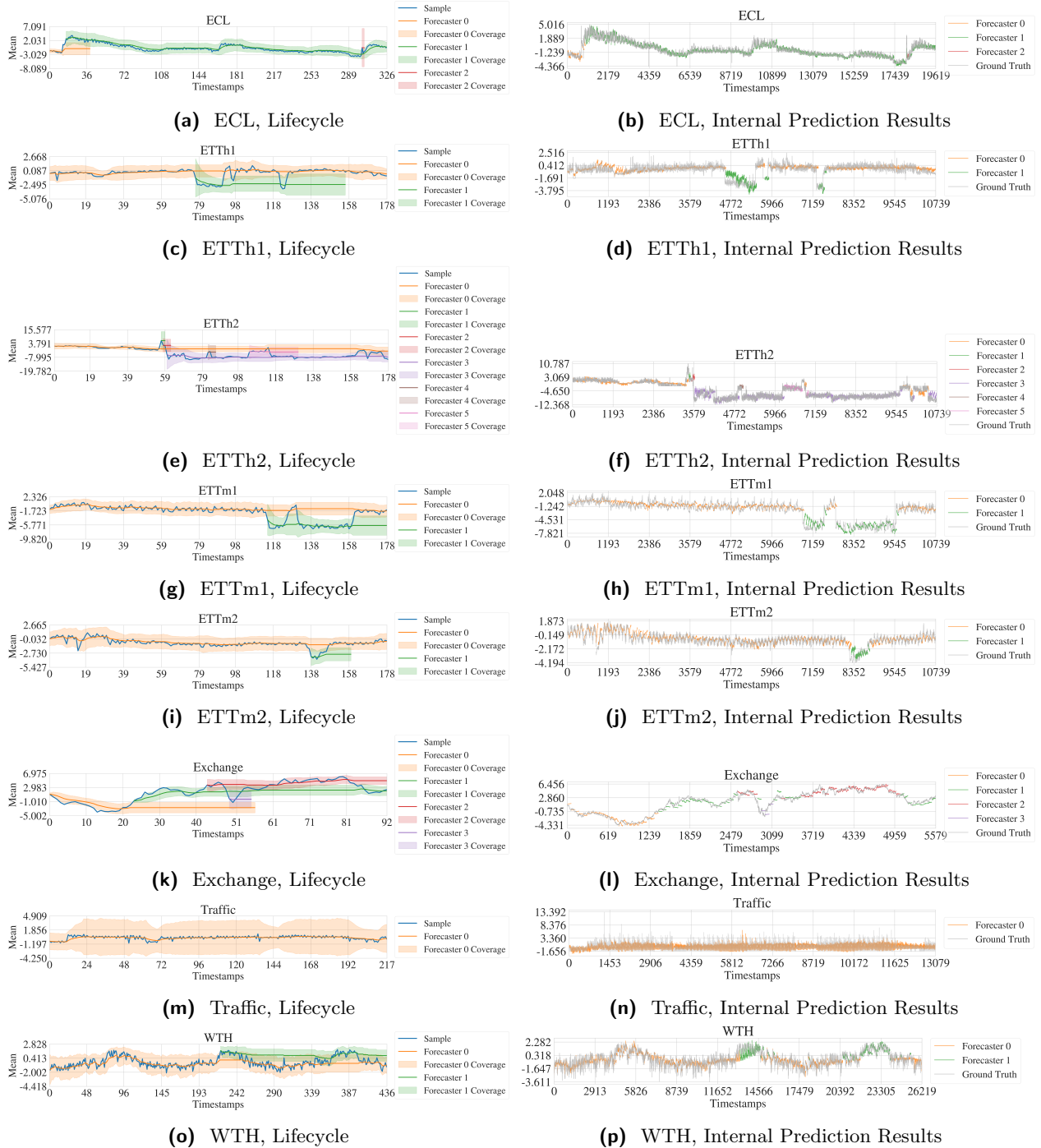


Figure 10 Visualization of forecaster gene trajectories.